Method Appendices

TIME DOMAIN ELECTROMAGNETICS
THE GEONICS EM61-MK2

Basic Methodology and Instrument Design
In order to generate EM fields, electrical current is passed through the lower coil and then turned off. After a short period of time the current is turned on again and the process repeated at 75 Hz. Turning on or off the current creates a changing EM field, and this forms the basis of the method.

When a changing EM field penetrates an object that conducts electricity, secondary electrical currents are induced to flow in the conductor. These currents then generate secondary changing EM fields that can be detected by a coil. These secondary EM fields are detected while the transmitter current is off. Secondary currents in highly conductive objects take longer to decay than do those in less conductive objects. Thus, the decay curves due to the conductivity of the ground decay relatively fast compared to those from metal objects. When no metal is present, a low-level or constant signal is received. An increased signal is received when metal is present. This signal is generally highest when the coils are located directly over the object, resulting in "bulls-eye" type anomalies for isolated metal objects and simplifies data analysis.

The EM61-MK2 uses electromagnetic (EM) fields (also called EM waves) to detect buried metallic objects. The instrument has two rectangular coils, 1.0 by 0.5 meters in size, mounted one above the other as shown in the figure on the right. The lower coil is the transmitter and also acts as a receiver and the upper coil is a receiver only. The instrument uses EM fields to locate buried metal, therefore any metal that conducts electrical current can be detected, including both ferrous and non-ferrous metal.

The EM61-MK2 allows the measurement of the secondary EM fields at certain times after the transmitter current has been turned off. These times are often called data channels, or time gates. These time gates are centered at approximately 216, 366, 660 and 1266 microseconds after the current has been turned

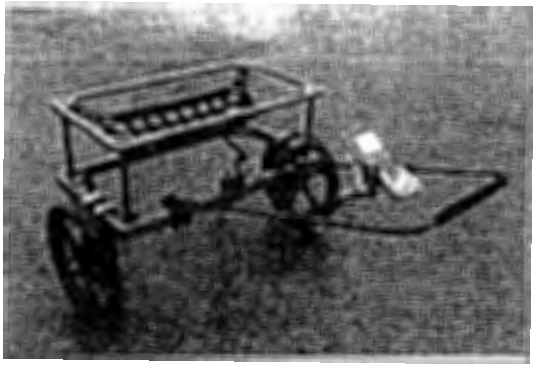

off. The top coil measures the secondary EM field 660 microseconds. The instrument provides the option to either measure all four times from the lower coil or the earliest three times from the lower coil and one reading from the top coil.

Field Data Recording
Data positioning may be accomplished using three different methods. The most accurate method of positioning the data involves the coupling of Global Positioning System (GPS) data with the geophysical data. GPS data is streamed directly into the recording console and merged with the geophysical data. Positioning of the data with GPS may result in a horizontal positional resolution of <5 cm. When using GPS for positioning, data are collected at user defined time intervals. The EM61-MK2 has the ability to collect up to 10 data points per second.

The other two methods are not as accurate and require additional work prior to surveying. One method uses an optical encoder housed in a single wheel of EM61. This method uses a predefined distance (rotation of the wheel) to collect data. Data collected in this manner normally have nominal along line-spacing of 0.63 feet. The final method allows for the collection of more data along the survey line but requires open areas for accurate positioning. This last method collects at user defined time intervals. This is the same mode of data collection as with GPS. During data acquisition marks are placed in the data. These marks are referenced to the survey grid and used to position the data during processing.

MAGNETIC SURVEYS

Introduction Magnetic surveys are conducted to evaluate geology, locate lava tubes in igneous rocks, find buried metal such as Underground Storage Tanks (UST) and pipelines and to locate Unexploded Ordnance (UXO).

The depth of investigation varies widely, depending on the target. Geologic structure can be determined to depths of many thousands of feet. UST's, pipelines and UXO targets are usually shallow. The method will probably only locate shallow lava tubes.

Basic Principles of the Magnetic Method
The magnetic field of the earth is a vector quantity and has, therefore, a direction and a magnitude. The shape of this field is that which would be produced if a large magnet were placed inside the Earth. Superimposed on this field are time varying fluctuations resulting from electrical activity in the ionosphere, usually caused by solar flares.

The Earth's magnetic field induces a secondary magnetic field in ferromagnetic objects, or geological structure that contains magnetite or other minerals that are magnetizable. This secondary magnetic field then "disturbs" the magnetic field of the earth creating an anomaly that can be detected with a magnetometer. Most magnetometers measure the magnitude of the magnetic field and can do so several times per second.

Figure 1 presents a schematic illustrating the magnetic field from a cylindrical ferromagnetic object. In this picture the Earth's field magnitude has been removed leaving only the magnitude of the field due to the ferromagnetic cylinder, often called the magnitude of the anomalous field.

Because the magnitude Earth's magnetic field changes with time, generally with daily cycles, called Diurnal changes, these changes have to be removed from the field data. In order to do this a base station is usually set up at a site near the survey area where magnetic anomalies are minimal. This instrument then records the magnitude of the magnetic field at regular intervals throughout the duration of the survey. This allows the diurnal variations in the magnetic field to be removed from the survey data during processing.

In addition to induced magnetization, remnant magnetization can also produce anomalies. Remnant magnetization occurs in geologic materials, usually volcanic and igneous rocks, which originate as hot

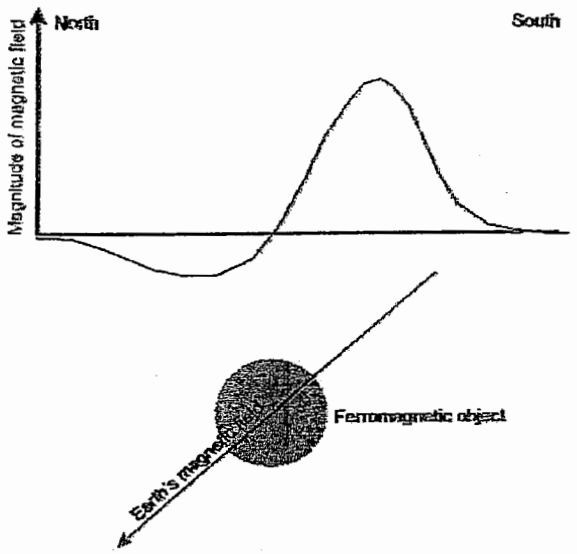

Figure 1
The Magnitude of the anomalous magnetic field created by a ferromagnetic cylinder in the presence of the Earth's field.

fluid lava and then cool before eventually solidifying. When the lava, or igneous material, cools below a temperature called the Curie point, the magnetic domains in the rock (usually magnetite) are oriented in the direction of the existing magnetic field at that time. Since the direction of the Earth's magnetic field changes over geologic time, the Remnant magnetic field can have a direction that is different from that produced by induction with the present Earth's magnetic field.

Field Data Recording
Magnetic surveys are conducted by first setting up a base station, as described above. The survey is then conducted by walking across the area of interest while the magnetometer records data, usually at several times per second. The data is stored in solid state memory in the instrument. In order to position the data, some magnetometers can be assembled with differential Global Positioning Systems (DGPS) allowing the spatial coordinates to be acquired simultaneously with the magnetic data. Conventional, or GPS, surveying of the ends of the lines may be required if DGPS data is not acquired with the magnetometer data. Linear interpolation methods can then be used to assign spatial coordinates to the data.

Interpretation

Magnetic data can be interpreted using computer software to model the anomalies. Generally, an initial model is developed for the source of the anomaly and the program then calculates the anomaly resulting from this source. The program then modifies the depth and geometry of the source and recalculates the anomaly. It does this until a reasonable fit is obtained between the field and model data. This process is called inversion.

Another interpretation method is to calculate a function called the Analytic Signal from the field data. Figure 2 illustrates this function for a cylindrical source along with the magnitude of the field (Anomaly Magnitude). Since the Analytic Signal peaks over the top of the source, the location of the source is easier to position than it is from the anomaly magnitude data. In addition, the amplitude of the Analytic Signal is related to the susceptibility of the source and the width is related to the depth to the top of the source.

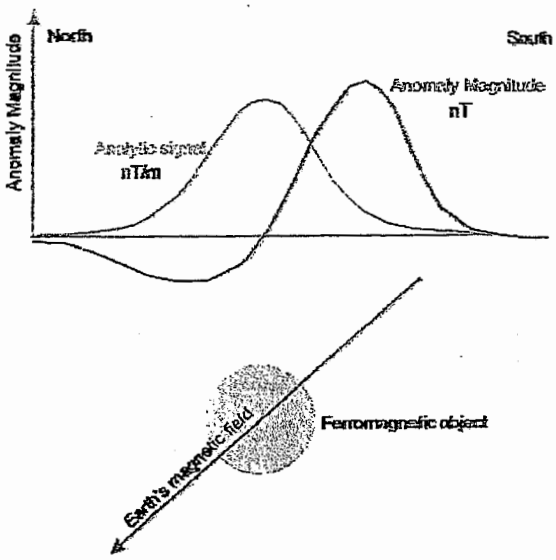

Figure 2
Anomaly magnitude and Analytic Signal over a ferromagnetic object.

Method Limitations

The magnetic method only detects objects composed of ferromagnetic materials, and not metals such as copper or aluminum. In interpreting magnetic data for geologic targets, there are generally several different solutions that can provide a theoretical fit of the field and model data, therefore each interpreted source is not necessarily unique. Such an interpretation is often called a "permissive" interpretation. This means that it is a valid theoretical interpretation but may be one of several possibilities. Non unique interpretations are not a concern when searching for buried ferromagnetic objects.

During severe magnetic storms, when the time varying magnetic field changes are significant, it may not be feasible to record field data.

Reprinted from
the Summer 1990 Issue of *Ground Water Monitoring Review*

Magnetic Surveying for Buried Metallic Objects

by Larry Barrows and Judith E. Rocchio

Abstract

Field tests were conducted to determine representative total-intensity magnetic anomalies due to the presence of underground storage tanks and 55-gallon steel drums. Three different drums were suspended from a non-magnetic tripod and the underlying field surveyed with each drum in an upright and a flipped plus rotated orientation. At drum-to-sensor separations of 11 feet, the anomalies had peak values of around 50 gammas and half-widths about equal to the drum-to-sensor separation. Remanent and induced magnetizations were comparable; crushing one of the drums significantly reduced both. A profile over a single underground storage tank had a 1000-gamma anomaly, which was similar to the modeled anomaly due to an infinitely long cylinder horizontally magnetized perpendicular to its axis. A profile over two adjacent tanks had a. smooth 350-gamma single-peak anomaly even though models of two tanks produced dual-peaked anomalies. Demagnetization could explain why crushing a drum reduced its induced magnetization and why two adjacent tanks produced a single-peak anomaly.

A 40-acre abandoned landfill was surveyed on a 50- by 100-foot rectangular grid and along several detailed profiles; The observed field had broad positive and negative anomalies that were similar to modeled anomalies due to thickness variations in a layer of uniformly magnetized material. It was not comparable to the anomalies due to induced magnetization in multiple, randomly located, randomly sized, independent spheres, suggesting that demagnetization may have limited the effective susceptibility of the landfill material. A different 6-acre site survey conducted on a 10- by 10-foot grid was analyzed to determine the maximum station spacing and line separation that could have been used. Essentially, all of the anomalies at this site would have been resolved by a survey conducted on a 20- by 20-foot grid and the larger anomalies would have been detected by a 50- by 50-foot grid.

Introduction

Magnetic surveys have traditionally been used by geologists to locate changes in rock type such as might be associated with ore bodies, fault contacts, or igneous intrusives. Another common application is determining the probable depth to basement beneath sedimentary rocks. For these applications, the principal geologic variable is the distribution of ferromagnetic minerals, mainly magnetite, within the earth. The theory and survey procedures are described in a variety of references (e.g., Grant and West 1965, S.E.G. 1966, Parasins 1975, Nettleton 1976, Telford and others 1977, Robinson and Coruh 1988). A particularly concise review of surveying with portable magnetometers is given by Breiner (1973).

Magnetic surveys are used in hazardous waste site investigations to locate 55-gallon drums, underground storage tanks, buried pipes, and the edges of covered landfills. These applications usually involve shallow iron or steel objects, which influence the way the surveys should be conducted and interpreted. Tyagi and others (1983) describe controlled field tests in which single drums and clusters of drums were buried at various depths. The test site was. then surveyed with a variety of geophysical instruments including a total intensity magnetometer. They found the magnetic detection limit for a single drum was 6 to 11 feet below the surface and that the boundaries of a dump site containing steel drums can be easily determined. Gilkeson and others (1986) describe a magnetic survey of a series of landfill trenches that had been used to dispose of steel drums. They found a distinctive pattern of magnetic highs over the trenches and lows over the intertrench corridors. They noted that these signals were similar to the calculated magnetic anomalies due to infinitely long rectangular bodies having dimensions comparable to the trenches and a magnetic susceptibility of $k = 0.1$. As explained later, a susceptibility of this magnitude is expected for a mass containing many disseminated ferrous metal objects. Frischknecht and others (1985) and Jachens and others (1986) describe field tests and models that demonstrate the use of magnetic surveys to locate covered abandoned well casings. This application is important because abandoned wells are potential pathways for the vertical migration of contaminated ground water. They found strong positive anomalies over the wells that closely resemble models of simple magnetic dipoles having the positive pole at the top of

the casing and the negative pole at its base.

In this paper, the theory behind magnetic surveying is briefly reviewed and the field tests conducted to determine the total-intensity magnetic anomalies due to 55-gallon steel drums and underground storage tanks are briefly described. The anomalies due to the three drums tested had peak amplitudes of around 50 gammas and half-widths approximately equal to the 11-foot separation between the drum and the magnetometer sensor. The half-width is the distance between the two sides of an anomaly at intensities of one-half of its peak value. These anomalies were similar to those due to isolated dipoles but in addition to the magnetization induced by the earth's ambient field, both remanent magnetization and demagnetization seemed to affect the signals. Remanent magnetization is a permanent magnetization that is independent of the ambient field. Demagnetization is a limit on the strength of induced magnetization within an object imposed by the internal field due to the object itself. The surveyed anomaly due to one underground storage tank was similar to that due to an infinitely long cylinder magnetized perpendicular to its axis. However, the anomaly due to two adjacent tanks also resembled that of a single body. Again, remanent magnetization and demagnetization are thought to affect these signals. If the results described herein are representative, then the strengths of anomalies due to drums and tanks may depend more on their volume than on their metal content. Also, it may be difficult to infer from the shape of a magnetic anomaly the exact location and nature of the causative body. Demagnetization may also influence the magnetic signals from landfills containing many metal objects. One site survey is described in which the total-intensity field resembled that due to a uniformly magnetized layer of varying thickness but did not resemble that due to an assembledge of magnetically independent objects. One implication is that magnetic surveys may not be able to locate concentrations of metal objects, such as drums, within a landfill. Another is that successful landfill surveys may be conducted on a relatively coarse station grid. The data from a second survey conducted on a 10- by 10-foot square grid were analyzed to determine the maximum station spacing that could have been used. For this particular site, essentially all of the signal would have been resolved with stations on a 20- by 20-foot grid and the stronger anomalies would have been detected on a 50- by 50-foot grid.

Theory

The Geomagnetic Environment

The signals in a magnetic survey are partially the result of, and strongly influenced by, the ambient magnetic field of the earth. As a first approximation this geomagnetic field resembles that due to a single axial dipole whose negative or south magnetic pole is toward the geographic north pole. The strength of this field varies from 60,000 gammas near the poles, where it plunges vertically into the ground, to 25,000 gammas near the equator where it parallels the earth's surface. In any particular region the ambient field is described by its intensity, inclination (or angle to the horizontal), and declination (or angle to geographic north). Breiner (1973) includes large-scale maps of these parameters for the continental United States. Fabino and others (1979) give more detailed maps.

The geomagnetic field is not constant both in the sense of diurnal variations of several tens of gammas and occasional periods of rapid, irregular, transient variations (magnetic storms). The diurnal variations can be removed from survey data by drift corrections based on either regular base station ties or the record from a fixed base-station magnetometer. Magnetic storms vary in intensity and can make surveying impractical. The Space Environment Services Division of the National Oceanic and Atmospheric Administration provides recorded information on the current level of these fluctuations (telephone number (303) 497-3235) and a forecast of the projected level for the next five days (telephone number (303) 497-3171). It is normally desirable to know the condition of the earth's field during each day of a field survey.

Magnetic Anomalies

Following Telford and others (1976, p. 111, Equation 3.11), the magnetic field at an external point (f, due to a magnetized body can be expressed as:

$$\vec{F}(\vec{r}_o) = \vec{\nabla} \int_{\text{volume}} \int \int \vec{M}(\vec{r}) \circledast \vec{\nabla} \frac{1}{|\vec{r} - \vec{r}_o|} \, dV(\vec{r})$$

where: $\vec{r}$ is a position vector within the body,
$\vec{\nabla}$ is the gradient operator,
$|\vec{r} - \vec{r}_o|$ is the distance between the external point and position within the body,
$\circledast$ indicates the vector dot product, and
$\vec{M}(\vec{r})$ is the net magnetization per unit volume.

The net magnetization is the vector sum of induced plus remanent magnetizations. Remanent magnetization is a permanent magnetic moment per unit volume and induced magnetization is temporary magnetization that disappears if the material is not in a magnetic field. Generally, the induced magnetization is parallel with and proportional to the inducing field. Algorithms for calculating the magnetic fields due to uniformly magnetized, simple geometric shapes are given in several texts (e.g., Grant and West 1965, Nettleton 1976, Telford and others 1976, Robinson and Coruh 1988).

Magnetic fields are vectors and magnetometers measure some attribute of this vector field. Proton precession magnetometers measure the maximum intensity (or total length of the vector) and flux gate magnetometers measure the intensity in a particular direction (or vector component). When used with dual sensors, magnetometers also measure the gradient of the attribute; usually in the vertical direction.

The net magnetic field to which the magnetometer responds is the vector sum of the field due to local magnetized materials and the ambient field of the earth. Figure 1 shows the total intensity field due to a simple magnetic dipole, the ambient field of the earth, and the total-intensity anomaly that would he detected during

a survey. In this case, the magnetization of the object is parallel to the ambient field (induced magnetization). There is a magnetic low to the north of the center of the body and a larger high to the south.

Effective Susceptibility

Magnetic susceptibility, k, is the dimensionless proportionality constant relating induced magnetization within a body to the inducing field. In general, the inducing field is the vector sum of both the earth's ambient field and the field due to the object itself. This feedback is referred to as demagnetization and is expressed as a reduction in the effective susceptibility of the object:

$$k_{eff} = \frac{k_{mat}}{1 + \lambda k_{mat}}$$

where: k_{mat}, is the material susceptibility, and A is the demagnetization factor. Grant and West (1965) describe the physical basis for demagnetization and the derivation of this relation.

Demagnetization factors are dependent on both the shape of the object and its orientation to the ambient field. For a sphere $\lambda = 4/3\ \pi$; normal to the axis of the cylinder $\lambda = 2\ \pi$; and normal to a flat sheet $\lambda = 4\ \pi$ (Strangway 1967). Figure 2 shows the resulting relations between effective and material susceptibility for these simple shapes and orientations. Note that for material susceptibility less than about k = 0.05, the effective and material susceptibilities are approximately equal. Most rock units have susceptibilities less than this, therefore, demagnetization does not usually affect the interpretation of geologic surveys. However, ferrous metals have susceptibilities of tens or hundreds, therefore, the effective susceptibility of ferrous metal objects, like steel drums, is limited by demagnetization to a few tenths. If the ferrous metal content of a landfill is several percent of the volume, then the effective susceptibility of landfill material would also be limited. In this case, local concentrations of metal within the landfill would not be expected to significantly increase the local effective susceptibility.

Demagnetization also limits the applicability of the algorithms used to calculate the magnetic effects of simple models. These algorithms usually assume that magnetization is uniform throughout the material, a condition not realized if the field due to the body itself is irregular. For hazardous waste site investigations there is a need to develop magnetic modeling techniques that accommodate demagnetization phenomena. Until this is accomplished, magnetic models of ferrous metal objects (including the models in this report) should be interpreted cautiously.

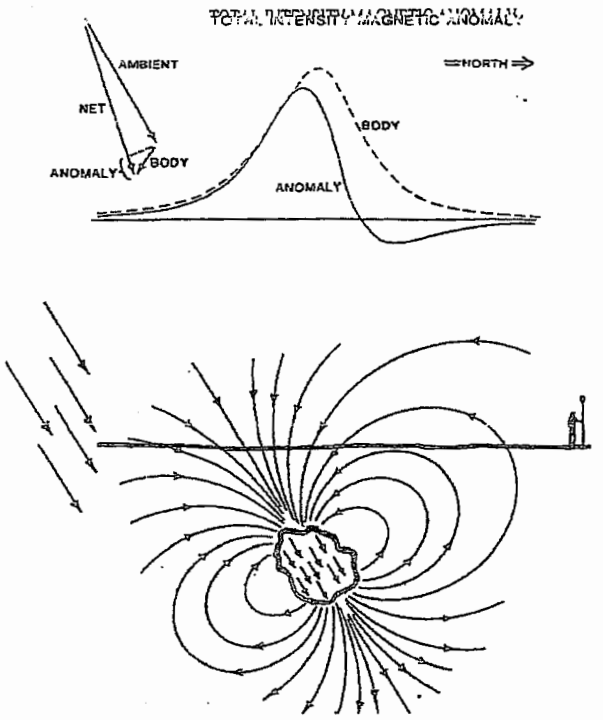

Figure L Magnetic effect of an isolated body magnetized in the direction of the earth's ambient field. The measured total magnetic intensity is the vector sum of the ambient field plus the field due to the body:

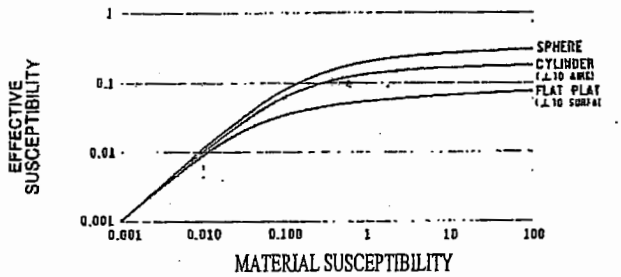

Figure 2. Effective vs. material susceptibility for several simple shapes and orientations. Demagnetization limits the effective susceptibility to a few tenths regardless of the susceptibility of the material (from Strangway 1967, p. 455).

Field Tests

55-Gallon Drums

The objectives of these tests were to establish the magnetic signal of a 55-gallon steel drum and to compare this result with analytical models. A secondary objective was to determine the extent to which demagnetization limits the effective susceptibility of a steel drum.

A 60- by 60-foot test site was laid out in a flat empty field and a nearby base station was selected. Survey stations were at 3-foot intervals along north-south lines, spaced 6 feet apart (231 stations). In the center of the site a non-magnetic (PVC pipe) tripod was constructed from which the drums were suspended. The drums were 19 feet above ground level; therefore, with the 8-foot sensor height of the magnetometer, the signals were similar to those from drums buried at 3 feet (Figure 3). Running the surveys beneath, instead of over, the objects reversed the signals through an east-west line. This resulted in a reversal of the positions of the positive peak and related trough.

The site was first surveyed with an empty tripod to establish a baseline, which was removed from all subsequent surveys. For each survey, the ends of the north-south lines were first read and linearly drift-corrected to the base station and then the individual stations were read and linearly drift-corrected to the line ends. All data were relative to the first reading at the base station

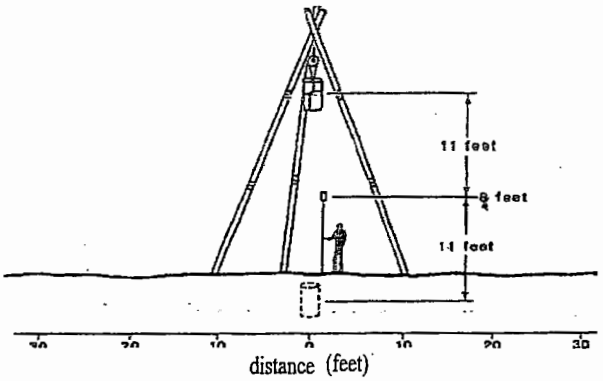

Figure 3. Test apparatus used to simulate the magnetic response of a buried 55-gallon steel drum. The anomaly due to the suspended drum is similar to that of a buried drum except that the positions of the high and low are reversed.

and all were gathered with a total intensity proton-procession magnetometer (Geometrics Model 856). **Figure 4 is a perspective diagram of a representative anomaly. The anomaly has a peak amplitude near 50 gammas, and has a half-width about equal to the drum-to-sensor separation (11 feet). It is less than 5 gammas at twice the separation.**

Tests were run with three different drums. For each drum, the field beneath the drum was surveyed, the drum was flipped and rotated to reverse the direction of the remanent magnetization, and the new field was surveyed. Along the north-south center line, the average of the two fields is attributable to induced magnetization and one-half their difference is attributable to remanent magnetization. For two of the three drums tested, the anomaly due to remanent magnetization was comparable to that due to induced magnetization. For the third drum, it was 40 percent as large.

The third drum was then crushed to a 1.1 cubic foot, drum-shaped mass. This crushed drum was surveyed in both its upright and reversed orientations. Figure 5 shows the observed data along the north-south central profile for both the whole and crushed drums in both of their orientations. In its crushed configuration, the drum showed very little remanant magnetization, possibly because the magnetized sheet metal had been folded over on itself. The anomaly due to induced magnetization was only 30 percent of that of the uncrushed drum even though both configurations contained the same steel.

Modeled profiles of the total intensity anomaly of uniformly magnetized spheres were matched to the induced-magnetization anomalies of both the whole and crushed drums. The sphere volumes were identical to their respective drums. For the whole drum, the modeled sphere had an effective susceptibility of $k = 0.10$, for the crushed drum $k = 0.18$.

Underground Storage Tanks

Magnetic surveys are used to locate underground storage tanks either for their removal or as an aid in positioning boreholes in which leak detectors are to be installed. The following field tests demonstrate the character of the associated total-intensity signals. Again, the data were gathered with a total-field proton-procession magnetometer.

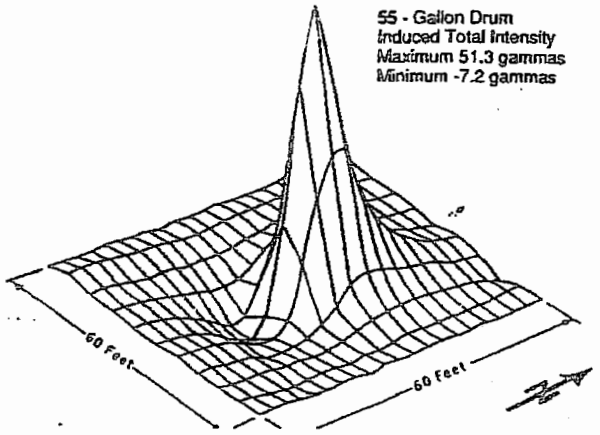

Figure 4. Total intensity anomaly due to induced magnetization in a single 55-gallon drum. The configured surface is one-half the sum of the anomaly due to a drum in its upright orientation plus that due to the same drum in a flipped plus rotated orientation. Survey stations were located at each of the grid intersections.

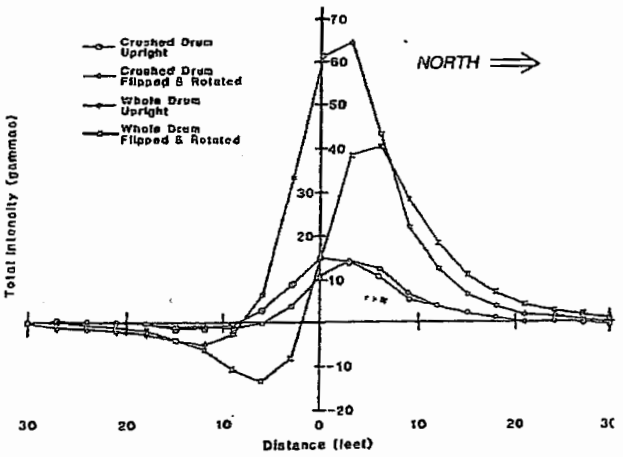

Figure 5. North-south profiles beneath a suspended 55-gallon drum in its upright orientation and its flipped plus rotated orientation. The lower-amplitude profiles are for the same drum after it had been crushed to a 1.1 cubic foot drum-shaped mass.

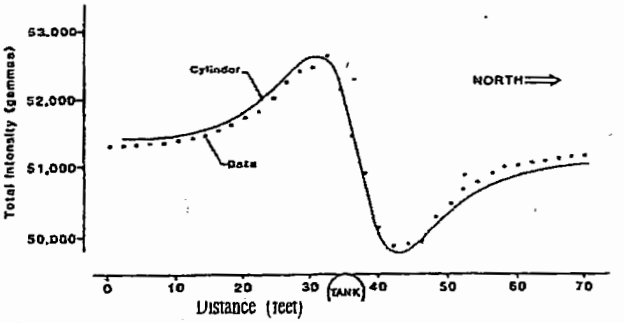

Figure 6. Total-intensity anomaly due to an underground storage tank. The modeled anomaly is that due to an infinitely long cylinder with a horizontal magnetization of 2750 gammas per cubic foot.

The first example is a single tank on a narrow land spit extending from the south shore of Lake Mead, Arizona. The tank had been part of a marine fuel dock until the facility was destroyed by high water and abandoned. There were no remaining buildings, power lines,

pipes or other sources of cultural noise.

Figure 6 is a profile normal to the long axis of this tank along with a matching model based on the actual tank diameter. The model has a uniform horizontal magnetization of 2750 gammas per unit volume. This net magnetization is the vector sum of induced plus remanent magnetization and cannot be resolved without reorienting the tank. One simple possibility is an induced magnetization of 5500 gammas per unit volume ($k = 0.1$) plus an upward remanent magnetization of 4763 gammas per unit volume.

The second example is a profile over two adjacent tanks located 22 feet to one side of a large vehicle maintenance garage. Figure 7 shows the observed data, an assumed linear regional, which may be due to the garage. and the residual anomaly along with the profile due to the indicated model. In this case, the entire anomaly might be due to induced magnetization in a single small body that is considerably deeper than the actual tanks. Note that the data did not resolve two tanks even though geometrically correct models of two magnetically independent tanks had dual-peaked anomalies. A possible explanation is that the inducing field within each tank is the sum of the earth's ambient field, the field due to the tank, and the field due to the adjacent tank. The tanks would then not be magnetically independent and the two-tank model would not apply.

Field Surveys

The Landfill

The first example is a survey of a 70-acre covered landfill in south-central Indiana. A 20-acre lake occupies the center of the site and a river flows along the northern and northeastern sides. The landfill had been used to dispose of approximately 40,000 drums of chemical wastes along with a variety of domestic and industrial refuse. The survey was conducted to better define the lateral extent of the landfill and, if possible. to locate clusters of drums.

Two survey methods were used. One was a reconnaissance survey with stations at 50-foot intervals along lines spaced 100 feet apart. The other was a series of more detailed north-south profiles with stations at 10- or 20-foot intervals. Both were conducted with GeoMetrics Model 856 total-intensity magnetometers.

Figure 8 is a contour map of the total intensity data from the reconnaissance survey. The dots are measurement stations and the contour interval is 1000 gammas. At this location, the ambient field is 56,200 gammas and the measured values range from 52,600 to 64.500 gammas, so the anomalous field ranges from 3600 to +8300 gammas. The reconnaissance survey clearly showed areas in the southeast corner and west-central side of the site that are magnetically smooth and are not believed to contain buried debris. The data contoured surprisingly well, considering that drums and metallic debris are exposed on the surface. At the relatively coarse 50- by 100-foot station spacing (necessitated by the size of the site and limited field time) many "single point anomalies" and ambiguities in the contours were anticipated.

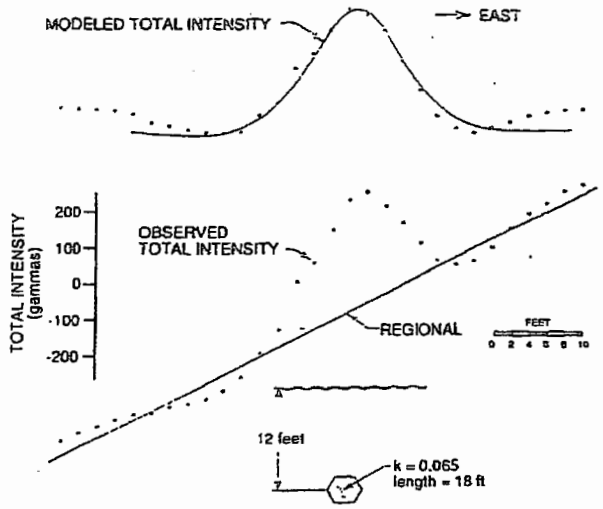

Figure 7. Total-intensity anomaly due to two underground storage tanks. The magnetic data did not resolve the presence of two objects even though calculated models of two near-surface magnetically independent tanks produced dual-peaked anomalies.

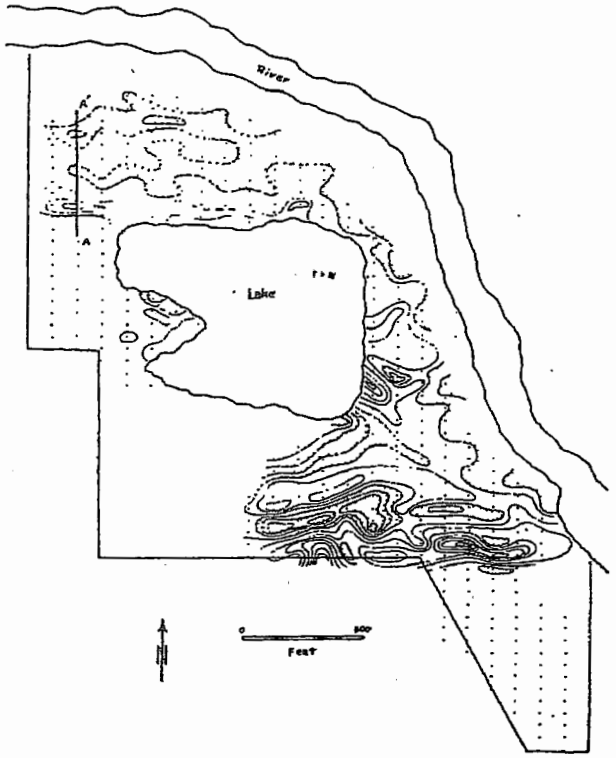

Figure 8. Magnetic total intensity over a covered landfill in south-central Indiana. The contour interval is 1000 gammas and the dots are stations at which data were gathered. Profile A-A' is shown in Figure 9.

The continuity of the contoured field may be due to demagnetization limiting and homogenizing the effective susceptibility of the landfill material. Figure 9 is a north-south profile along line A-A. Stations are at 10-foot intervals. Also shown is a simple model and modeled field configured to match the larger features in the observed data. The model is an east-west trending, infinitely long polygon with a uniform susceptibility of $k = 024$ (the Talwanii algorithm, e.g., Grant and West 1965). The horizontal scale is as shown, but there is a lOX vertical exaggeration in the model and its greatest

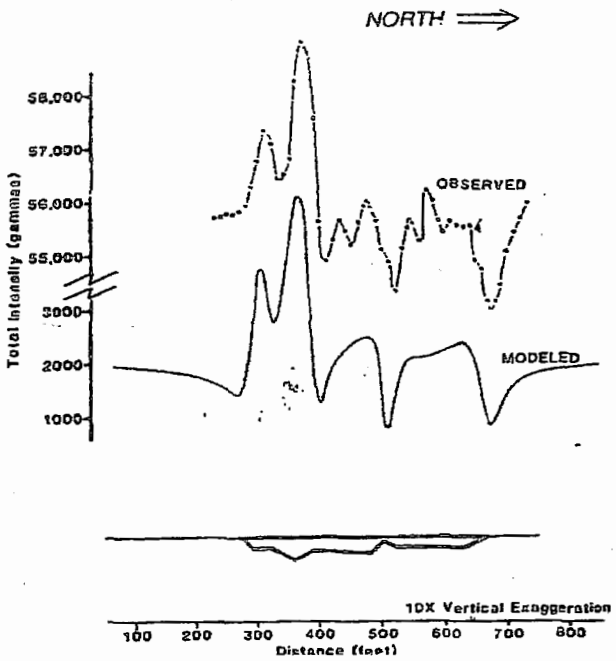

Figure 9. Observed and modeled magnetic total intensity over a covered landfill. The modeled anomalies are due to variations in the configuration of the landfill material.

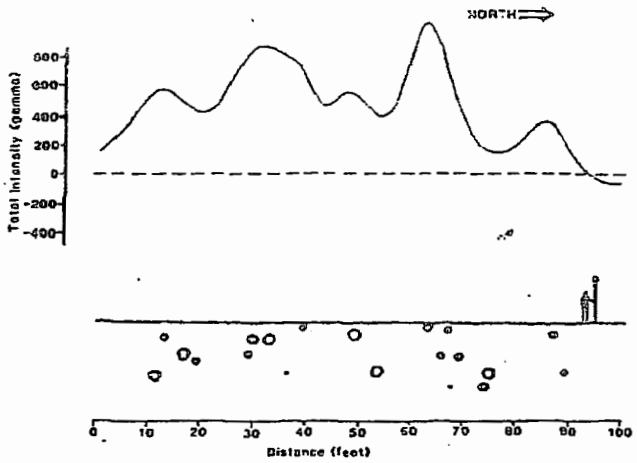

Figure 10. A total-intensity magnetic model of an assembledge of randomly located, randomly sized spheres magnetized in the direction of the earth's field. The modeled field is dominated by a few narrow peaks due to the shallowest objects.

thickness is only 5 feet. The important point is that the anomalies can be attributed to modest thickness variations in the layer. Comparable results were obtained with models having an irregular upper surface and a flat base. In contrast, Figure 10 shows the effect of induced magnetization in an assembledge of randomly located, randomly sized spheres. This modeled field is predominately positive and dominated by a few high-intensity narrow peaks due to the shallowest objects. The observed field at the landfill had broad anomalies with both positive and negative parts.

The Sludge Ponds

The next example is a survey of some abandoned sludge ponds on a 6-acre site south of Houston, Texas. The ponds had been used to dispose of broken slabs of reinforced concrete and had then been covered with earth. The survey objective was to locate areas where the slabs had been dumped so they could when drilling ground water monitoring wells. It was thought that the steel reinforcing bars in the concrete

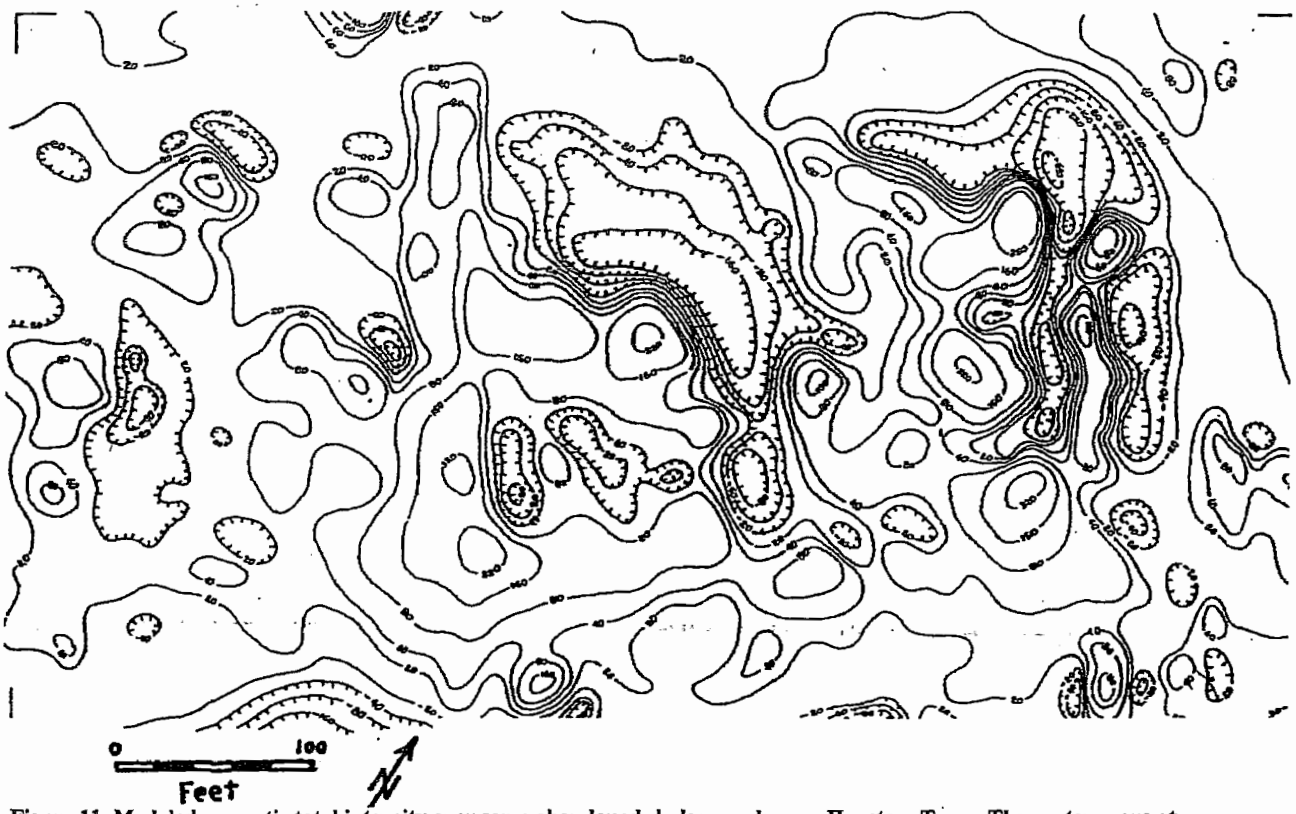

Figure 11. Modeled magnetic total intensity over some abandoned sludge ponds near Houston, Texas. The contours are at 49800 ± 20, ± 40, ± 80, ±160, ± 320, ± 640 gammas and stations were on a 10- by 10- foot square g rid.

would produce a detectable magnetic anomaly.

This survey was conducted with an OMNI-IV tie-line magnetometer system. Stations were established at 10-foot intervals along lines 10 feet apart and both the total intensity and its vertical gradient were recorded. The OMNI-IV monitors the quality of each reading and the data are reliable except in an 80-foot strip along the eastern side of the site where there is an overhead powerline. In this area about 20 percent of the readings were unreliable and were edited from the data.

Figure 11 is a contour map of the edited total intensity data. Values range from 49,150 to 50,350 gammas. The ambient field at this location is 49,800 gammas so the anomalies range from -650 to +550 gammas. The exponentially spaced contour intervals were used so that both subtle features in the relatively smooth areas and the shapes of the larger anomalies are displayed. This map along with a map of the vertical gradient sucessfully identified undisturbed areas in which the monitoring wells could be placed.

On Figure 11 there is a tendency for the magnetic highs to be flanked to the north by lows of comparable amplitude. As in the landfill survey, the effect could be modeled as thickness variations in a continuous layer. However, at this site, enough of the slab dumps (and anomalies) are sufficiently isolated to suggest a different interpretation. Figure 12 shows the total intensity anomaly due to a horizontally magnetized slab at a depth of 4 feet. For horizontal magnetization at the latitude of the site, the magnetic highs and lows are of comparable amplitude but for steeply plunging magnetization parallel to the ambient field, the highs are significantly larger than the lows. Demagnetization limits the effective susceptibility perpendicular to the surface of a slab or to the axis of a bar. However, it does not limit the susceptibility parallel to a thin slab or along the axis of a bar. Therefore, for flat-lying reinforced slabs, the horizontal component of induced magnetization is expected to be larger than the vertical component, which is consistent with our model.

Selecting station spacing and line separation involves a tradeoff between survey resolution and the amount of field work. If the distance between measurements is too large, the data will be uncertain by an amount comparable to the amplitude of the narrower anomalies; even if the measurements are precise. (This spatial-aliasing phenomena is similar to the temporal aliasing that occurs when a continuous time signal is digitized.) On the other hand, if the distance between measurements is too small, the time and cost of the survey may be prohibitive. For the survey over the sludge ponds, the relatively short 10- by 10-foot grid was selected because the nature of the signal was not known beforehand and the surveyor wanted to detect all significant anomalies.

To determine the maximum distance between stations that would have adequately resolved the field variations, the Fourier transformation was used on the total intensity data and then the resulting amplitude spectra (Figure 13) was smoothed and contoured. This map shows the relative amplitudes of the variations in magnetic total intensity as a function of their widths

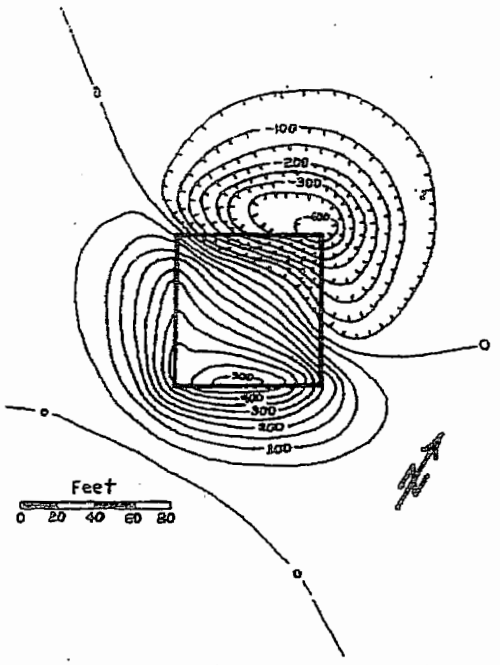

Figure 12. Magnetic total intensity anomaly due to a 80- by 80- by 4-foot thick slab of material with a horizontal northerly magnetization of 1000 gammas per cubic foot. The contour interval is 50 gammas.

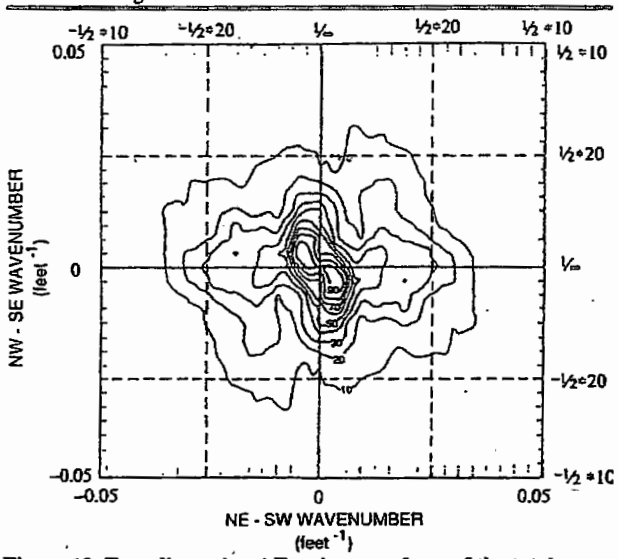

Figure 13. Two-dimensional Fourier transform of the total intensity data in Figure 11. The contoured values are the moduli of the transform after they were smoothed by a nine-point unit matrix. The contour interval is 10 percent of the maximum value.

and orientations. The graph axes are wave number or one-half the reciprocal wavelengths in the ENE-WSW and NNW-SSE directions of the survey grid. The contours are the moduli of the transform (an array of complex numbers) after they had been filtered or averaged with a nine-point unit matrix. The contour interval is 10 percent of the peak filtered value.

Note that almost all of the amplitude spectra are at wavenumbers less than 0.025 ft (0.5/20 ft). This implies that most features would be adequately resolved by a survey conducted on a 20-foot grid, assuming the data were reliable. Some data redundancy is desirable and it is more efficient to make closely spaced readings along

more widely separated lines than it is to make the same number of readings on a square grid. An optimum survey grid at this site might have stations at 10-foot intervals along lines no more than 30 feet apart. Contour maps constructed from alternate stations and lines (a 20- by 20-foot grid) and from every third line (a 10- by 30-foot grid) resolved all of the anomalies on the total-intensity map.

The highest peaks on the amplitude spectra occur at wave numbers near 0.005 ft (0.5/100 feet) and amplitudes are generally less that 50 percent of the peak value at wave numbers greater than about 0.01 ft (0.5/50 ft). This implies that the larger amplitude anomalies would have been detected by a survey on a 50-foot grid. A map constructed from every fifth line and station detected all the major anomalous areas but did not resolve the shapes of the anomalies.

Summary

Magnetic surveys can be an important part of hazardous waste site investigations but the physical principles must be understood before the data are interpreted. In particular, these surveys often involve ferrous metals and effective susceptibility can be limited by demagnetization to a few tenths. The magnetic field variations will then be due to the configuration of the magnetized material rather than to local concentrations of metal.

The detectable anomaly due to an isolated steel drum has a width of about twice the distance between the drum and the magnetometer sensor. A survey to reliably detect single drums would have to be conducted with a station spacing and line separation less than this width. However, if a hazardous waste site contains sufficient disseminated metal for demagnetization to occur, the stronger anomalies can have dimensions comparable to the landfill cells. In this case, relatively coarse station spacings and line separations may be adequate.

Acknowledgments

The landfill survey in south-central Indiana was conducted by Mike Gibbons and Aldo Mazzella for the U.S. Environmental Protection Agency. The drum study was conducted by the authors, also with support from the U.S. EPA. The study of underground storage tanks was part of a Boy Scout service project by Mike Barrows and the sludge pond survey was conducted by Jerry Robinson for the ENSR Corp. The contributions of all these individuals and agencies is gratefully acknowledged.

References

Breiner, S. 1973. Applications Manual for Portable Magnetometers: GeoMetrics, Sunnyvale, California.

Fabiano, E.B., W.J. Jones, and N.W. Peddie. 1979. The Magnetic Charts of the United States for Epoch 1975: U.S. Geological Survey-Circular 810, 15 p.

Frischknecht, EC. and P.V. Raab.1985.Location of abandoned wells with geophysical methods: NTIS Report PB 85-122638, National Technical Information Service. S[P]rin[g]field. Virginia, 48 p.

Gilkeson, R.H., P.C. Heigold and D.E. Laymon. 1986. Practical application of theoretical models to magnetometer surveys on hazardous waste disposal sites — A case history. *Ground Water Monitoring Review,* v. 6, n. 1, pp. 54-61.

Grant, F.S. and G.F. West. 1965. *Interpretation Theory in Applied Geophysics.* McGraw-Hill, New York. pp. 306-381.

Jachens, R.C., M.W. Webring, and EC. Frischknecht. 1986. Abandoned-well study in the Santa Clara Valley, California. U.S. Geological Survey, Open-File Report 86-350, 13p.

Nettleton, L.L. 1976. *Gravity and Magnetics in Oil Prospecting.* McGraw-Hill, New York, pp. 305-426.

Parasnis, D.S. 1986. *Mining Geophysics.* Elsevier Scientific Publishing Co., Amsterdam, pp. 3-60.

Robinson, E.S. and C. Coruh. 1988. *Basic Exploration Geophysics.* J. Wiley & Sons, New York, pp. 333-444.

Soc. of Exp. Geophysicists (eds). 1967. *Mining Geophysics,* v. II. Soc. of Exp. Geophysicists, Tulsa, Oklahoma, pp. 423-620.

Strangway, D.W. 1967. *Magnetic Characteristics of Rocks.* 1967. Soc. of Exp.Geophysicists, pp. 454-473.

Telford, W.M., L.P. Geldart, R.E. Shrift, and D.A. Keys. 1976. *Applied Geophysics.* Cambridge University Press, Cambridge, pp. 105-217.

Tyagi, S., A.E. Lord Jr., and R.M. Koerner. 1983. Use of a proton precession magnetometer to detect buried drums in sandy soil. *Jour. of Hazardous Materials,* v. 8, pp. 11-23.

Biographical Sketches

Larry Barrows received his M.S. and Ph.D. degrees in geophysics from the Colorado School of Mines in 1973 and 1978, respectively. He has worked as a systems engineer on Skylab remote-sensing experiments and as an exploration geophysicist in frontier areas of Alaska. Since 1979 he has specialized in geophysical surveying for ground water and hazardous waste site investigations, first as the project geophysicist on a radioactive waste disposal program and then as a research scientist for the U.S. EPA. In 1988 he joined Earth Science and Engineering Inc and LaCoste and Romberg Gravity Meters Inc (4807 Spicewood Springs Rd, Bldg. 2, Austin TX 78759). Current projects include using microgravity to detect solution conduits in karst terrains and using seismic groundroll to determine near-surface shear moduli.

Judith E. Rocchio is the future air resource specialist on the Stanislaus National Forest (1977 Greenley Rd, Sonora, CA 95370). She will obtain the position upon completion of her M.A. degree in air resource management at Colorado State University, Department of Natural Resources (1990). She was with Lockheed Engineering Management Services Co., Las Vegas, Nevada, prior to attending CSU where she was involved in several environmental monitoring programs and co-authored the paper with Dr. Barrows. From 1981 to 1986 Rocchio was a project geologist for Gower Oil Co. and Consolidation Coal Co., Denver, Colorado. She received her B.S. in geology (1981) from the University of Nevada, Las Vegas.

Magnetic Survey Anomaly Investigation Results – July 2007

Location #	Result
1	Unused USGS Caisson
2	12" piece of rebar
3	Nail
4	Rock
5	Rock
6	2' x 2' steel plate
7	Rock
8	Rock
9	Nail
10	Rock
11	Rock
12	Bolt
13	Rock
14	Nail
15	Wire
16	Steel roller
17	Bolt
18	Steel roller
19	Pipe
20	Steel plate
21	Rock
22	Rock
23	Bolt
24	Open end wrench
25	Steel roller
26	Nail
27	Bungee hooks
28	Bungee hook

All items were excavated using a backhoe and isolated using a Schonstedt Magnetic Locator.

ATTACHMENT 3

SUPPLEMENTAL ENGINEERING CALCULATIONS

SLOPE STABILITY VERIFICATION

AquAeTer

optimizing environmental resources - water; air; earth

CALCULATION SUMMARY SHEET

PROJECT NUMBER: 073113

PROJECT NAME: USEN – Trench 12 Design, Supplemental Calculations

DATE: September 18, 2007

CALCULATION NUMBER: _____ Revision: Update per 2007 Design

CALCULATION TITLE: Deep Seated Slope Stability Revision

DESCRIPTION OF CALCULATION:

Calculation to re-evaluate the stability of the final cell 12 cover configuration for pseudo-static loading conditions considering revised surface soil thicknesses and waste cohesion values.

REFERENCES USED: Number of Reference Pages Attached: _____

1. Previous Calc: 1996 Calculation titled "Deep Seated Slope Stability – Final Configuration"
2. Modeling Program: WinStabl Version 2.40

REVIEW COMMENTS:

CALCULATION MADE BY: SLW DATE: 9/18/2007

CALCULATION CHECKED BY: CAB DATE: 9/18/2007

CALCULATION REVISED BY: _____ DATE: _____

CALCULATION REVIEWED BY: SLW DATE: 9/18/2007

Purpose of Slope Stability Verification Calculation

Loose Soil Layer Thickness. Calculations and related information documenting the 1996 Design, as previously accepted by the NDEP, appear to include some inaccuracy in the description of the loose surface soil layer in the Trench 12 area. In various parts of the information, this layer is described as being as little as four and as much as 20 feet thick. The "Geotechnical Investigation for Cell 12" by Grant Environmental (July 1994) gives the loose surface soil layer as 4.0, 9.0, 4.0, and 8.0 feet thick on the south, east, north, and west sides of Trench 12, respectively. Considering these thickness values, which were determined by consideration of all deep boring data available in the Trench 12 area indicate that two general thickness conditions represent the loose surface soil layer – these are 5.0 feet thick and 10.0 feet thick. These two thicknesses are used in slope stability calculations done (in a manner similar to that used for the 1996 calculations) to determine the sensitivity of slope stability to certain soil properties.

Soil and Waste Strength. Stability analyses for the 1996 Design, as revised and later accepted by NDEP, indicate that the loose surface soil layer should be improved to achieve a cohesive strength of 1,000 PSF. Considering the thickness of that layer (i.e., from 5.0 to 10.0 feet) and the geometry of potential slope failures, the previous specification for surface material improvement could be too conservative. This revised calculation shows that the cohesion of reworked surface soil is not critical to achieving acceptable slope stability.

Waste properties appear to be more important to final cover slope stability than creating a small strong wedge in the surface soil layer. Also, some waste properties (cohesive strength and unit weight) considered in the 1996 Design calculations appear to be overly conservative with regard to slope stability.

- The assumed cohesive strength of waste is adjusted to 550 PSF, which is only slightly higher than the 500 PSF assumed for the 1996 Design calculations. The 1996 calculations provide justification (copied and included in this calculation from "Enclosure C to Attachment 1 of the December 1996 Response to NOD") for using hazardous waste cohesion values from 575 to 900 PSF. This minor adjustment in the assumed waste property is both justifiable and remains a conservative assumption.

- The unit weight of the upper portion (above ground level) of the hazardous waste that will be disposed in Trench 12 is adjusted to 100 PCF from the value of 115 PCF used for the 1996 Design calculations. The actual unit weight of waste disposed by US Ecology in Trench 11 is 96.3 PCF. Adjusting the waste weight to 100 PCF is justified by actual site waste disposal records.

Slope Stability Analysis Method

The computer modeling program WinStabl, using the Modified Bishop Method of analysis, was used to assess slope stability when varying the thickness of the loose soil layer and the cohesive strength of the waste in the final Trench 12 configuration. The Modified Bishop Method also

was used for the slope stability analyses in the 1996 Design. The model accepts as input the material properties (principally, unit weight, cohesive strength, and angle of internal friction) and a set of coordinates defining the position of the materials in typical Trench 12 cross-sections. The model is then asked to find deep seated failure surface through the various layers. For these analyses, a pseudo-static condition is assumed to represent seismic loading. The output of the model is calculated factors of safety for the identified failure surface and materials.

Analysis

The following conditions were considered in this slope stability verification.

1. Excavation sidewall slopes with a 10-feet thick surface soil layer.
2. Final soil cover (closed Trench 12) with 5-feet thick improved surface soil wedge.
3. Final soil cover (closed Trench 12) with 10-feet thick improved surface soil wedge.

Excavation slopes with 10-feet thick surface soil layer

For excavation slope stability, the 10-feet thick layer of unimproved surface soil zone (loose soil, cohesion = 0 PSF) is the 'worst case condition'. Slope stability analyses considering failure surfaces within each of the soil types present in the Trench 12 subsurface, including the surface soil layer, show that that factors of safety against slope failure under pseudo-static loading (simulating design earthquake loads) are much greater than 1.0. Slope stability under the 'worst case' operating condition (i.e., fully excavated trench, no waste in place) is acceptable.

Final soil cover (closed Trench 12)

The influence of variations in the properties of the improved surface soil wedge at both 5.0 and 10.0 feet thickness are the conditions under which slopes in the waste fill and natural or improved surface soil must be stable. Various configurations of material properties and slope failure surfaces were evaluated to determine which properties are significant to slope stability and which properties, if any, should be improved on trench construction to achieve acceptable stability.

The following table lists the various conditions analyzed and the resulting factor of safety for the following slope conditions:

Improved Surface Soil Wedge Thickness (feet)	Improved Surface Soil Wedge Cohesion (PSF)	Waste Cohesion (PSF)	Waste Weight (PCF)	Pseudo-Static Loading (g)	Factor of Safety
5 feet					
5	0	500	115	0.42	0.94

Improved Surface Soil Wedge Thickness (feet)	Improved Surface Soil Wedge Cohesion (PSF)	Waste Cohesion (PSF)	Waste Weight (PCF)	Pseudo-Static Loading (g)	Factor of Safety
5	250	500	115	0.42	0.95
5	1000	500	115	0.42	0.99
5	250	550	115	0.42	0.98
5	500	550	115	0.42	0.99
5	250	600	115	0.42	1.00
5	500	600	115	0.42	1.02
5	250	500	100	0.42	0.99
5	**250**	**550**	**100**	**0.42**	**1.02**
10 feet					
10	0	500	115	0.42	0.98
10	250	500	115	0.42	1.00
10	250	550	115	0.42	1.02
10	250	600	115	0.42	1.05
10	**250**	**550**	**100**	**0.42**	**1.04**

PSF = pounds per square foot
PCF = pounds per cubic foot
Bold = final condition with acceptable strength and stability

Results

To be acceptable, the factors of safety against slope failure under pseudo-static loading conditions (i.e., 0.42 g, which simulates the maximum horizontal acceleration value with a 90 percent or greater probability of not being exceeded in 250 years, NAC 444.6793) should equal or exceed 1.0.

For the 5-feet thick surface soil layer, representing the north and south sides of Trench 12, the condition that meets or exceeds the slope stability requirement is a surface soil layer with a cohesion of 250 PSF or greater; a waste cohesion of 550 PSF or greater, and a waste weight of 100 PCF or less. When the waste weight of 100 PCF (approximately the same as the actual Trench 11 average disposed waste weight of 96.3 PCF) is considered, the surface soil cohesion needed is 250 PSF and waste cohesion needed is 550 PSF.

For the 10-feet thick surface soil layer, representing the east and west sides of Trench 12, the condition that meets or exceeds slope stability requirements is a surface soil layer with a cohesion of 250 PSF or greater, a waste cohesion of 550 PSF or greater, and a waste weight of

100 PCF or less. When the waste weight of 100 PCF (approximately the same as the actual Trench 11 average disposed waste weight of 96.3 PCF) is considered, the surface soil cohesion needed is 250 PSF and waste cohesion needed is 550 PSF.

In both sets of slope evaluations, acceptable slope stability is achieved with the surface soil layer cohesion at 250 PSF, a value shown by laboratory soil tests to be achievable with recompaction of the natural surface soil with little or no addition of fine materials. These analyses show that the Trench 12 slopes, during and after operations (i.e., initial excavation slopes and final cover slopes), are acceptably stable without improving the cohesive strength of the surface soil layer (wedge) to a value greater than 250 PSF.

WIN STABL

MODEL RUNS

Typical excavation slope, with 0.42 g horizontal acceleration

	Moist Unit Weight	Saturated Unit Weight	Isotropic Strength Intercept	Isotropic Strength Angle
1	120.00	120.00	250.00	35.00
2	120.00	120.00	0.00	35.00
3	120.00	120.00	1440.00	35.00
4	120.00	120.00	2880.00	35.00
5	120.00	120.00	2160.00	35.00
6	120.00	120.00	4320.00	35.00

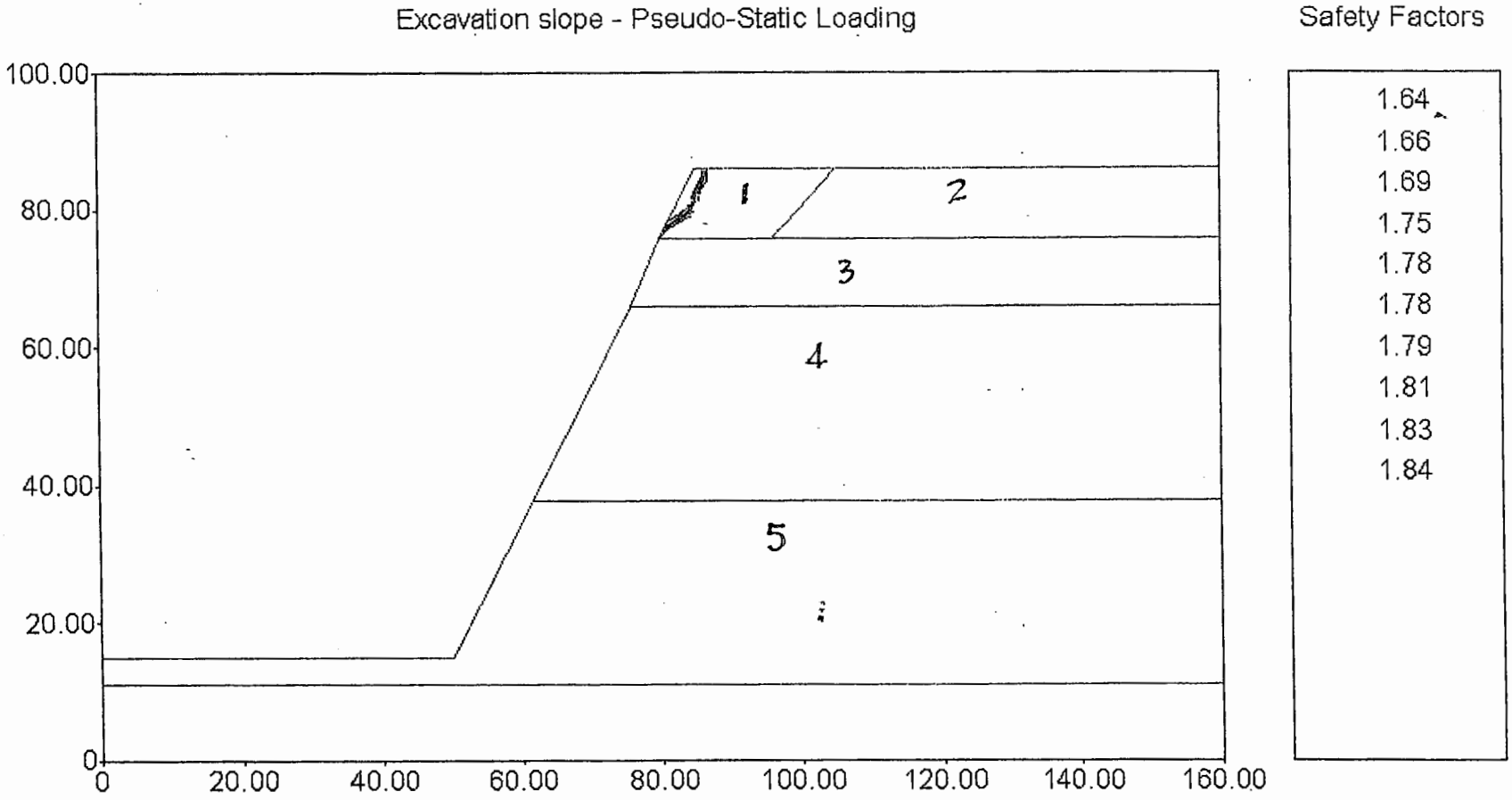

Typical excavation slope, with 0.42g horiz. acceleration

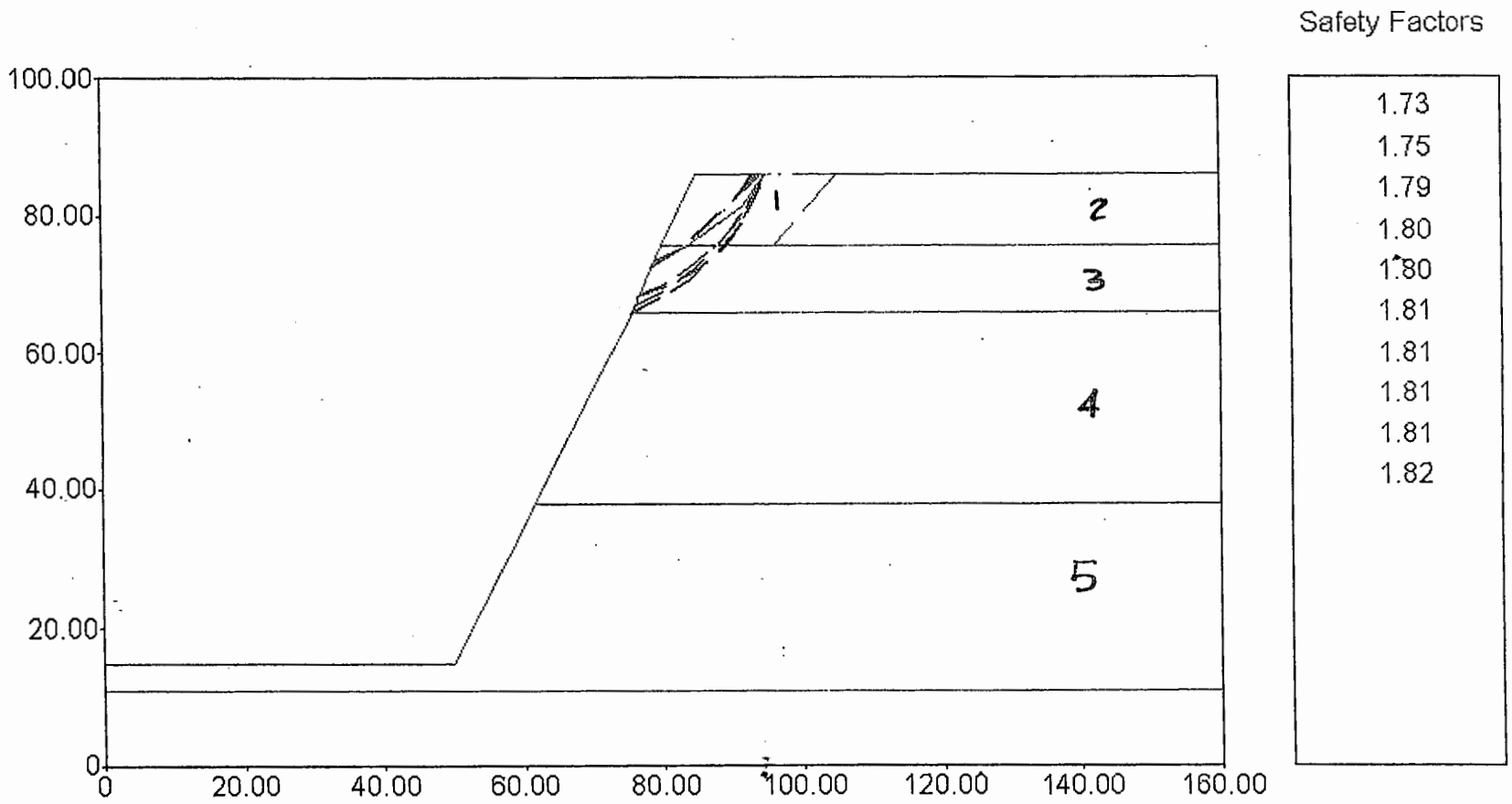

Typical excavation slope, with 0.42g horiz. acceleration

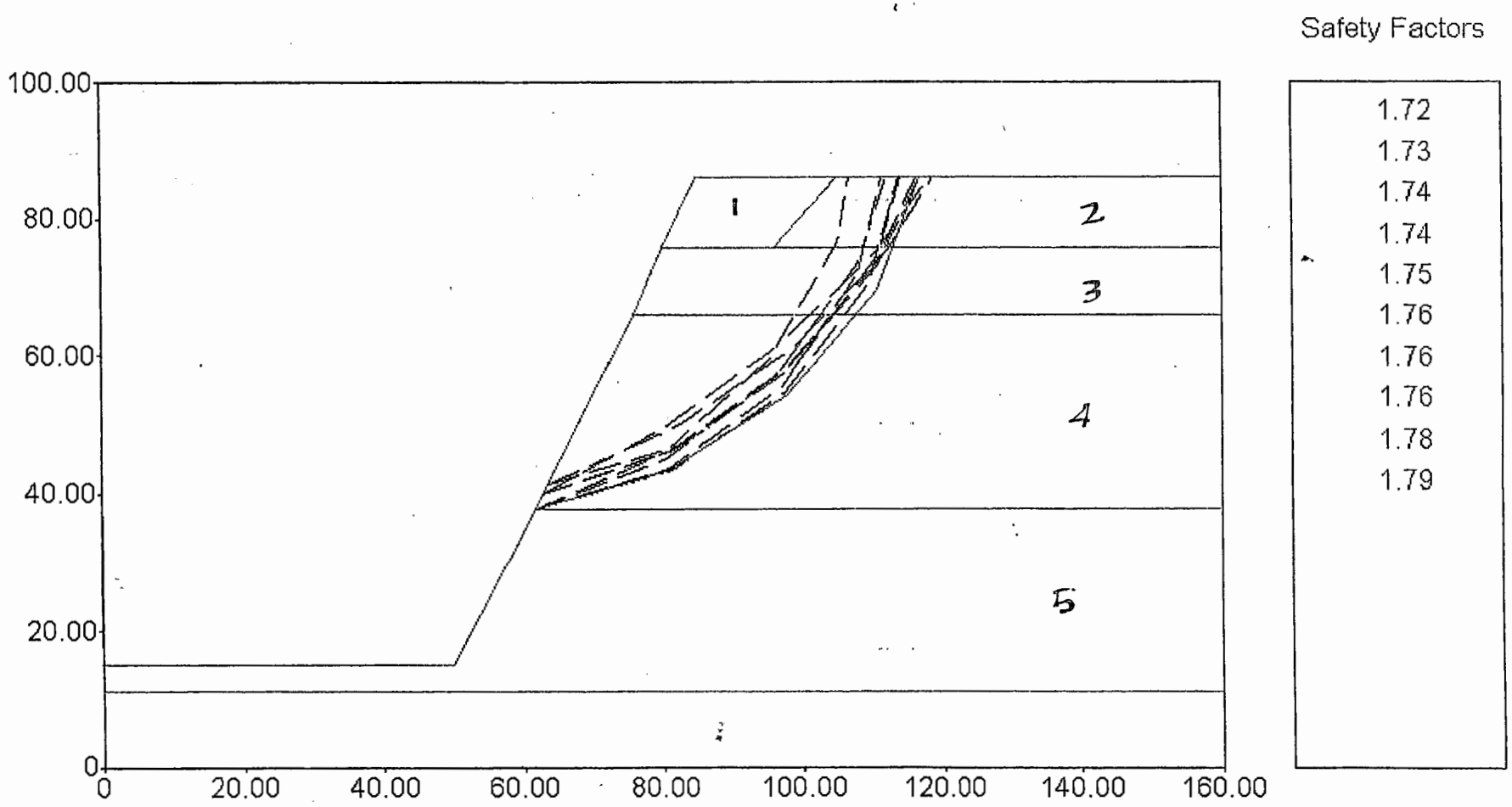

Typical excavation slope, with 0.42g horiz. acceleration

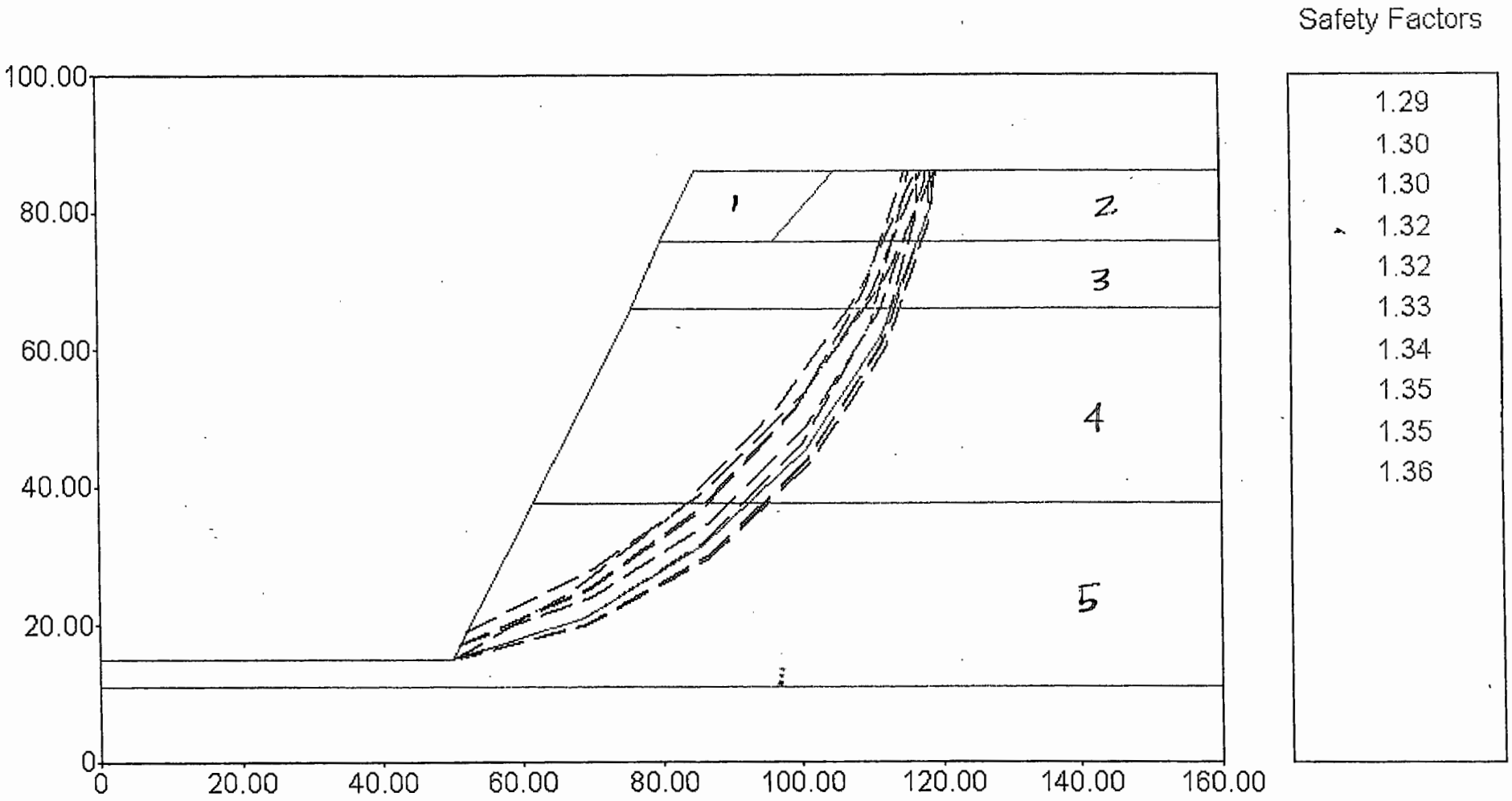

Profile.out
** PCSTABL6 **

by
Purdue University

modified by
Peter J. Bosscher
University of Wisconsin-Madison

--Slope Stability Analysis--
Simplified Janbu, Simplified Bishop
or Spencer's Method of Slices

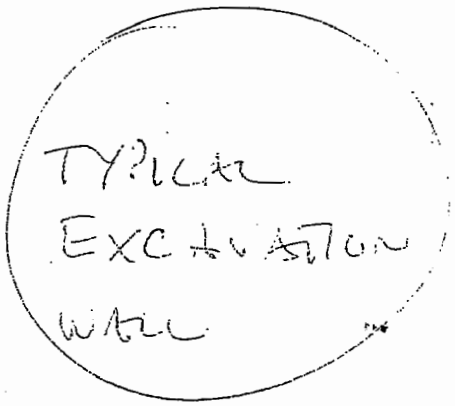

PROBLEM DESCRIPTION

BOUNDARY COORDINATES

7 Top Boundaries
13 Total Boundaries

Boundary No.	X-Left (ft)	Y-Left (ft)	X-Right (ft)	Y-Right (ft)	Soil Type Below Bnd
1	0.00	15.00	50.00	15.00	5
2	50.00	15.00	62.00	38.00	5
3	62.00	38.00	76.00	66.00	4
4	76.00	66.00	80.00	76.00	3
5	80.00	76.00	85.00	86.00	1
6	85.00	86.00	105.00	86.00	1
7	105.00	86.00	160.00	86.00	2
8	80.00	76.00	96.00	76.00	3
9	96.00	76.00	105.00	86.00	2
10	96.00	76.00	160.00	76.00	3
11	76.00	66.00	160.00	66.00	4
12	62.00	38.00	160.00	38.00	5
13	0.00	11.00	160.00	11.00	6

ISOTROPIC SOIL PARAMETERS

6 Type(s) of Soil

Soil Type No.	Total Unit Wt. (pcf)	Saturated Unit Wt. (pcf)	Cohesion Intercept (psf)	Friction Angle (deg)	Pore Pressure Param.	Pressure Constant (psf)	Piez. Surface No.

1	120.0	120.0	250.0	35.0	0.00	0.0	0
2	120.0	120.0	0.0	35.0	0.00	0.0	0
3	120.0	120.0	1440.0	35.0	0.00	0.0	0
4	120.0	120.0	2880.0	35.0	0.00	0.0	0
5	120.0	120.0	2160.0	35.0	0.00	0.0	0
6	120.0	120.0	4320.0	35.0	0.00	0.0	0

A Horizontal Earthquake Loading Coefficient
Of0.420 Has Been Assigned

A Vertical Earthquake Loading Coefficient
Of0.000 Has Been Assigned

Cavitation Pressure = 0.0 psf

A Critical Failure Surface Searching Method, Using A Random Technique For Generating Irregular Surfaces, Has Been Specified.

100 Trial Surfaces Have Been Generated.

10 Surfaces Initiate From Each Of 10 Points Equally Spaced Along The Ground Surface Between X = 79.00 ft.
and X = 82.00 ft.

Each Surface Terminates Between X = 85.00 ft.
and X = 87.00 ft.

Unless Further Limitations Were Imposed, The Minimum Elevation At Which A Surface Extends Is Y = 0.00 ft.

5.00 ft. Line Segments Define Each Trial Failure Surface.

Following Are Displayed The Ten Most Critical Of The Trial Failure Surfaces Examined. They Are Ordered - Most Critical First.

* * Safety Factors Are Calculated By The Modified Janbu Method * *

Failure Surface Specified By 4 Coordinate Points

Point No.	X-Surf (ft)	Y-Surf (ft)
1	80.33	76.67
2	84.14	79.91
3	86.63	84.25
4	86.95	86.00

*** 1.639 ***

Failure Surface Specified By 4 Coordinate Points

Point No.	X-Surf (ft)	Y-Surf (ft)
1	80.67	77.33
2	84.66	80.34
3	86.68	84.92
4	86.93	86.00

*** 1.664 ***

Failure Surface Specified By 4 Coordinate Points

Point No.	X-Surf (ft)	Y-Surf (ft)
1	80.33	76.67
2	84.08	79.98
3	86.21	84.50
4	86.94	86.00

*** 1.693 ***

Failure Surface Specified By 4 Coordinate Points

Point No.	X-Surf (ft)	Y-Surf (ft)
1	80.33	76.67
2	84.62	79.24
3	85.86	84.09
4	86.83	86.00

*** 1.754 ***

Failure Surface Specified By 4 Coordinate Points

Point No.	X-Surf (ft)	Y-Surf (ft)
1	80.00	76.00
2	83.90	79.14
3	86.25	83.55

4	86.36	86.00

*** 1.778 ***

Failure Surface Specified By 4 Coordinate Points

Point No.	X-Surf (ft)	Y-Surf (ft)
1	80.00	76.00
2	83.55	79.53
3	86.13	83.81
4	86.62	86.00

*** 1.778 ***

Failure Surface Specified By 4 Coordinate Points

Point No.	X-Surf (ft)	Y-Surf (ft)
1	80.33	76.67
2	84.43	79.54
3	85.91	84.31
4	86.34	86.00

*** 1.793 ***

Failure Surface Specified By 4 Coordinate Points

Point No.	X-Surf (ft)	Y-Surf (ft)
1	80.67	77.33
2	84.95	79.92
3	86.39	84.70
4	86.59	86.00

*** 1.812 ***

Failure Surface Specified By 4 Coordinate Points

Point No.	X-Surf (ft)	Y-Surf (ft)
1	81.00	78.00
2	85.00	81.01

3	86.78	85.68
4	86.80	86.00

*** 1.826 ***

Failure Surface Specified By 4 Coordinate Points

Point No.	X-Surf (ft)	Y-Surf (ft)
1	80.33	76.67
2	84.02	80.04
3	86.89	84.14
4	86.92	86.00

*** 1.842 ***

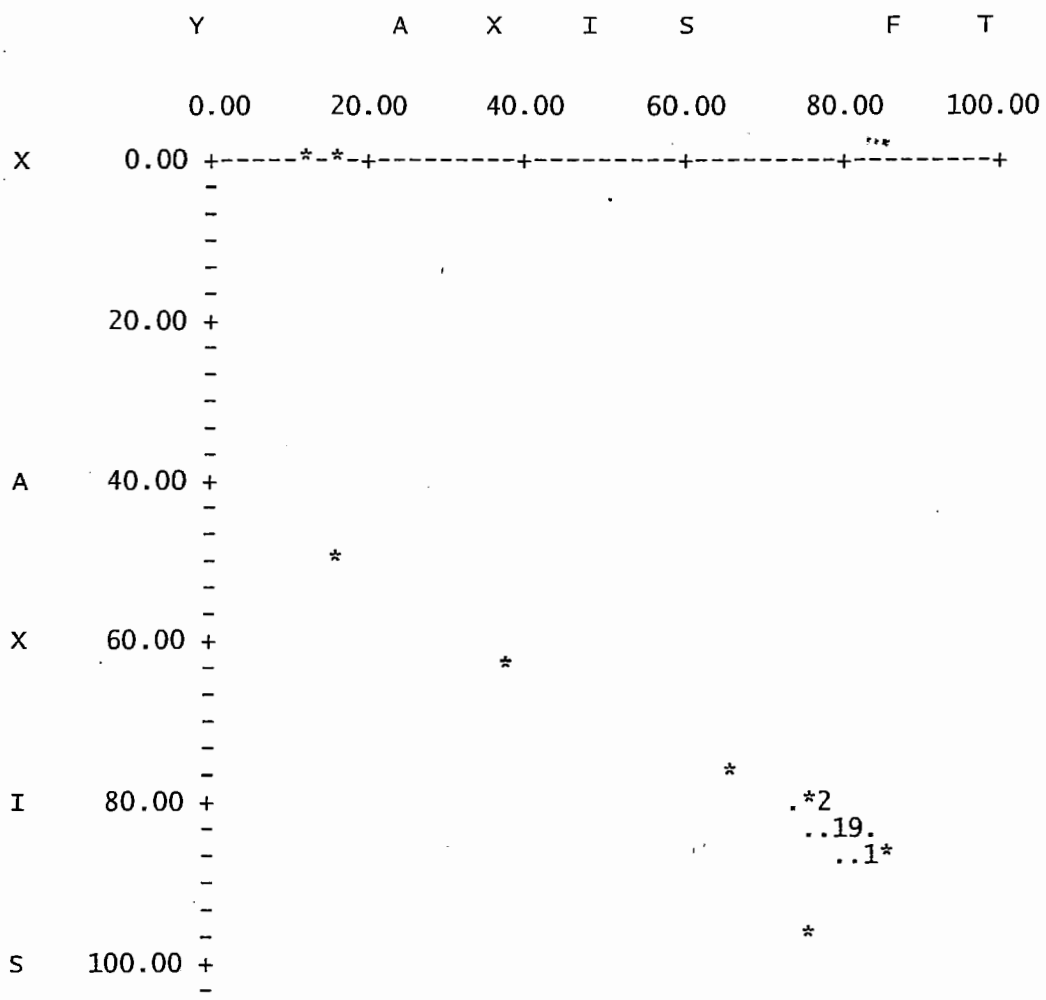

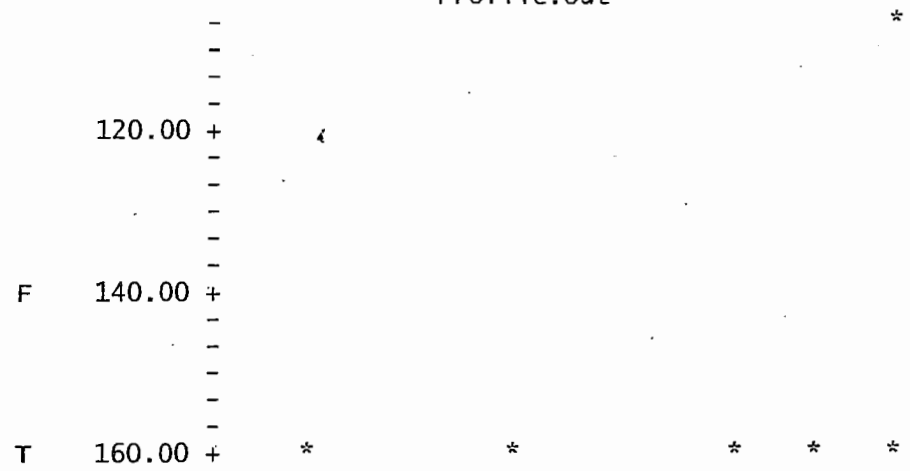
120.00
F
140.00
T
160.00

Final Cover Slope Stability for section with 5 feet of surface soil

Surface soil at C = 0 PSF (not recompacted)

Waste at C = 500 PSF

	Moist Unit Weight	Saturated Unit Weight	Isotropic Strength Intercept	Isotropic Strength Angle
1	120.00	120.00	0.00	35.00
2	115.00	115.00	500.00	27.00
3	120.00	120.00	1000.00	35.00
4	115.00	115.00	500.00	27.00
5	120.00	120.00	0.00	35.00
6	120.00	120.00	0.00	35.00
7	120.00	120.00	1440.00	35.00
8	120.00	120.00	2880.00	35.00
9	120.00	120.00	2160.00	35.00
10	120.00	120.00	4320.00	35.00

Pseudo-Static loading (0.42 g) for 5-ft thick surface soil layer

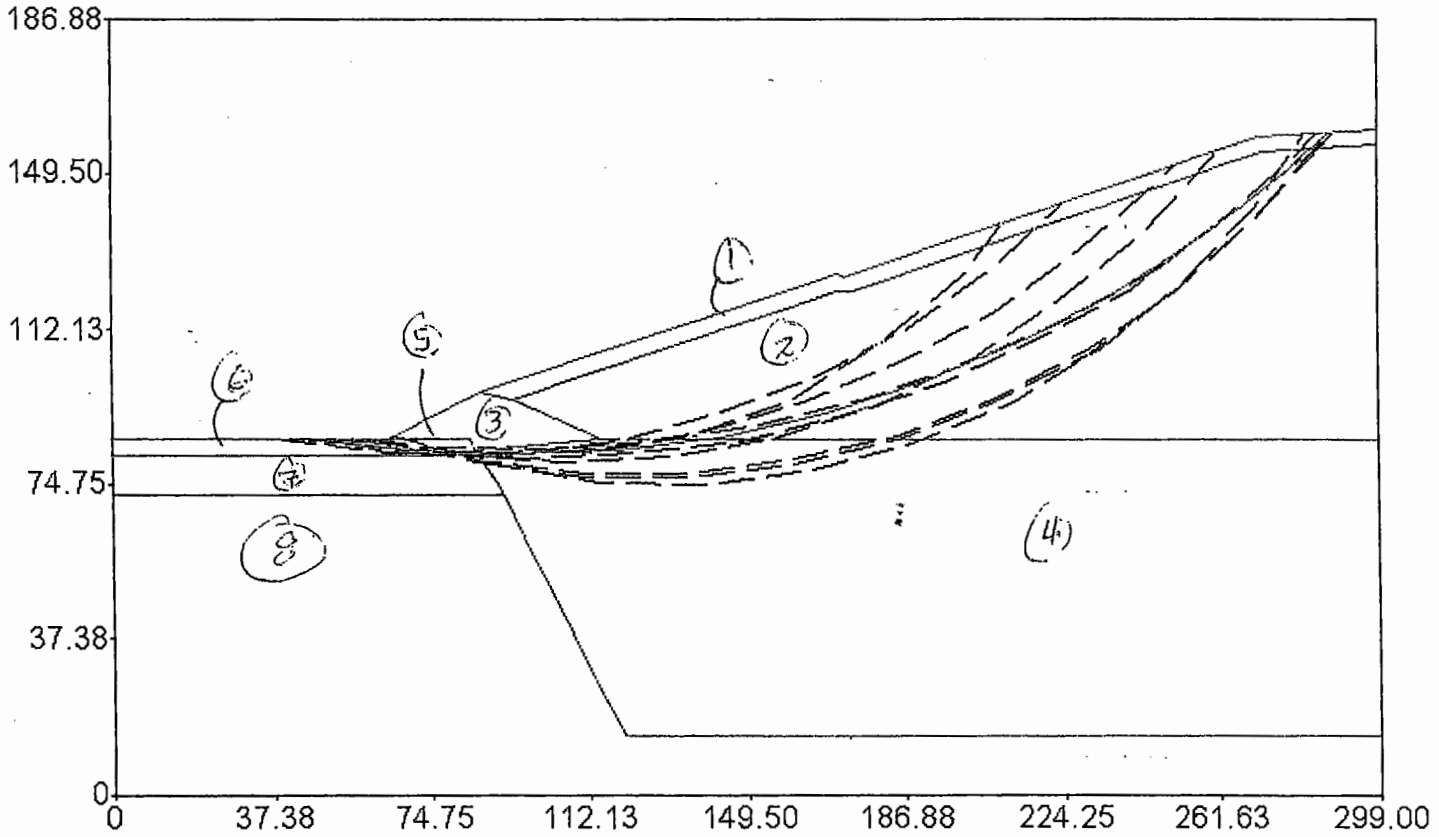

Safety Factors

0.94
0.94
0.95
0.98
0.98
0.98
0.99
1.01
1.02
1.04

Final Cover Slope Stability for section with 5 feet of surface soil

Surface soil at C = 250 PSF (recompacted, no amendment)

Waste at C = 500 PSF

	Moist Unit Weight	Saturated Unit Weight	Isotropic Strength Intercept	Isotr Strength Angle.
1	120.00	120.00	0.00	35.00
2	115.00	115.00	500.00	27.00
3	120.00	120.00	1000.00	35.00
4	115.00	115.00	500.00	27.00
5	120.00	120.00	250.00	35.00
6	120.00	120.00	0.00	35.00
7	120.00	120.00	1440.00	35.00
8	120.00	120.00	2880.00	35.00
9	120.00	120.00	2160.00	35.00
10	120.00	120.00	4320.00	35.00

Pseudo-Static loading (0.42 g) for 5-ft thick surface soil layer

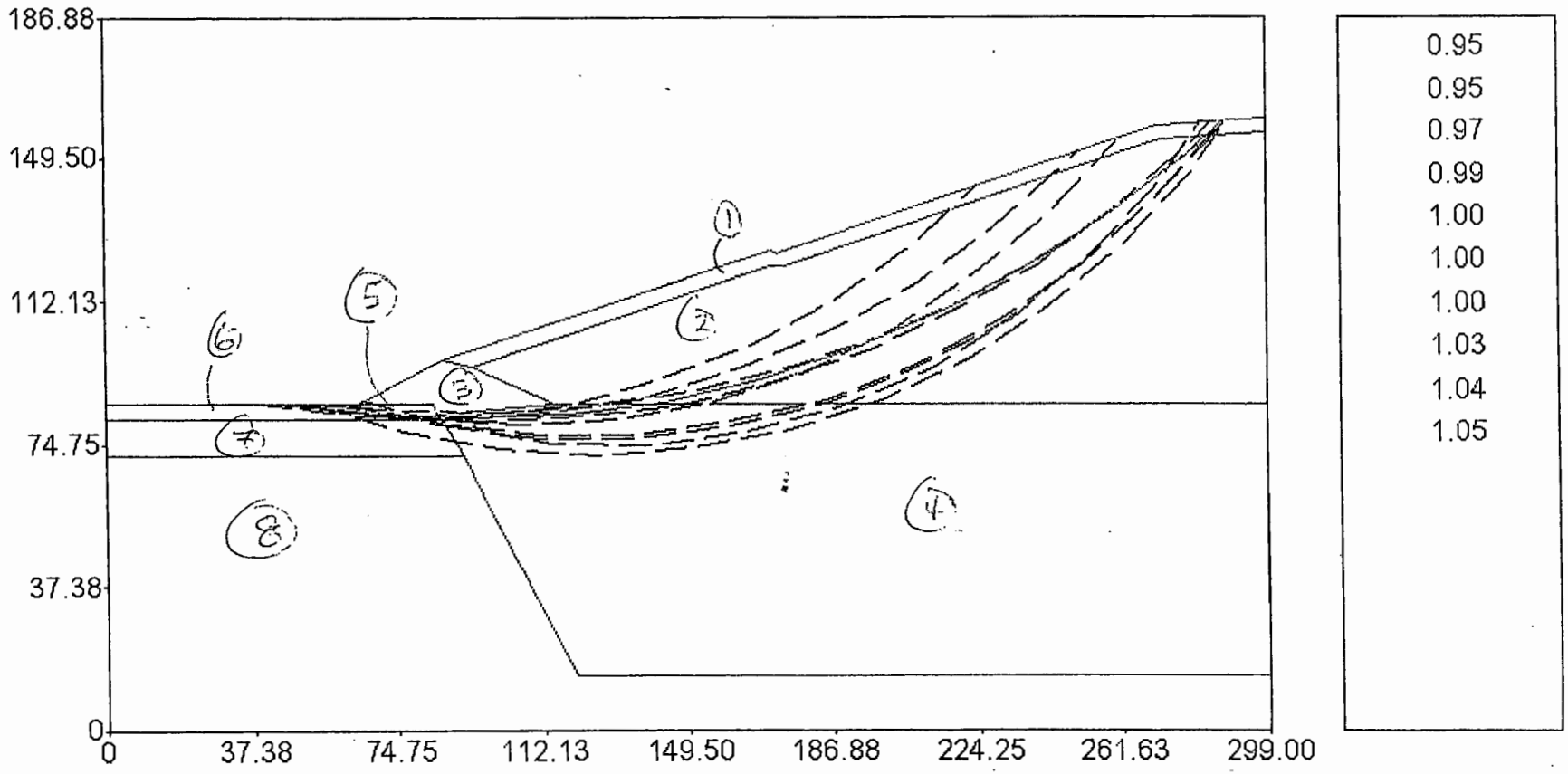

Safety Factors

0.95
0.95
0.97
0.99
1.00
1.00
1.00
1.03
1.04
1.05

Final Cover Slope Stability for section with 5 feet of surface soil.

Surface soil at C = 1000 PSF (Recompacted, with additives)

Upper waste at 115 PCF weight, C = 500 PSF (cohesion)

Lower waste at 115 PCF weight, C = 500 PSF (cohesion

	Moist Unit Weight	Saturated Unit Weight	Isot Stre.. Intercept	sotropic trength Angle
1	120.00	120.00	0.00	35.00
2	115.00	115.00	500.00	27.00
3	120.00	120.00	1000.00	35.00
4	115.00	115.00	500.00	27.00
5	120.00	120.00	1000.00	35.00
6	120.00	120.00	0.00	35.00
7	120.00	120.00	1440.00	35.00
8	120.00	120.00	2880.00	35.00
9	120.00	120.00	2160.00	35.00
10	120.00	120.00	4320.00	35.00

Pseudo-Static loading (0.42 g) for 5-ft thick surface soil layer

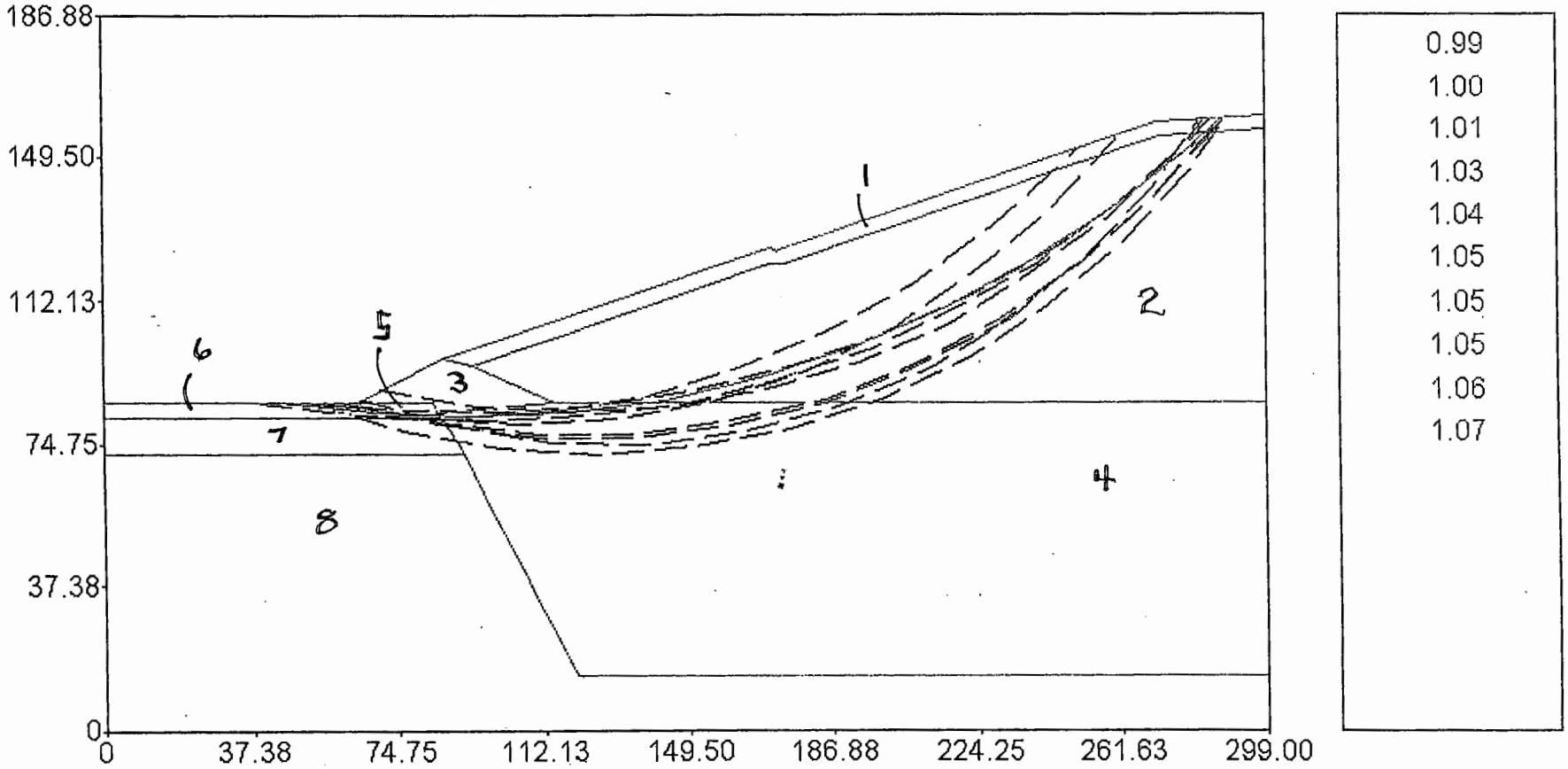

Safety Factors

0.99
1.00
1.01
1.03
1.04
1.05
1.05
1.05
1.06
1.07

Final Cover Slope Stability for section with 5 feet of surface soil

Surface soil at C = 250 PSF (recompacted, no amendment)

Waste at C = 550 PSF

	Moist Unit Weight	Saturated Unit Weight	Isotro(Strengt.. Intercept	tropic .rength Angle
1	120.00	120.00	0.00	35.00
2	115.00	115.00	550.00	27.00
3	120.00	120.00	1000.00	35.00
4	115.00	115.00	550.00	27.00
5	120.00	120.00	250.00	35.00
6	120.00	120.00	0.00	35.00
7	120.00	120.00	1440.00	35.00
8	120.00	120.00	2880.00	35.00
9	120.00	120.00	2160.00	35.00
10	120.00	120.00	4320.00	35.00

Pseudo-Static loading (0.42 g) for 5-ft thick surface soil layer

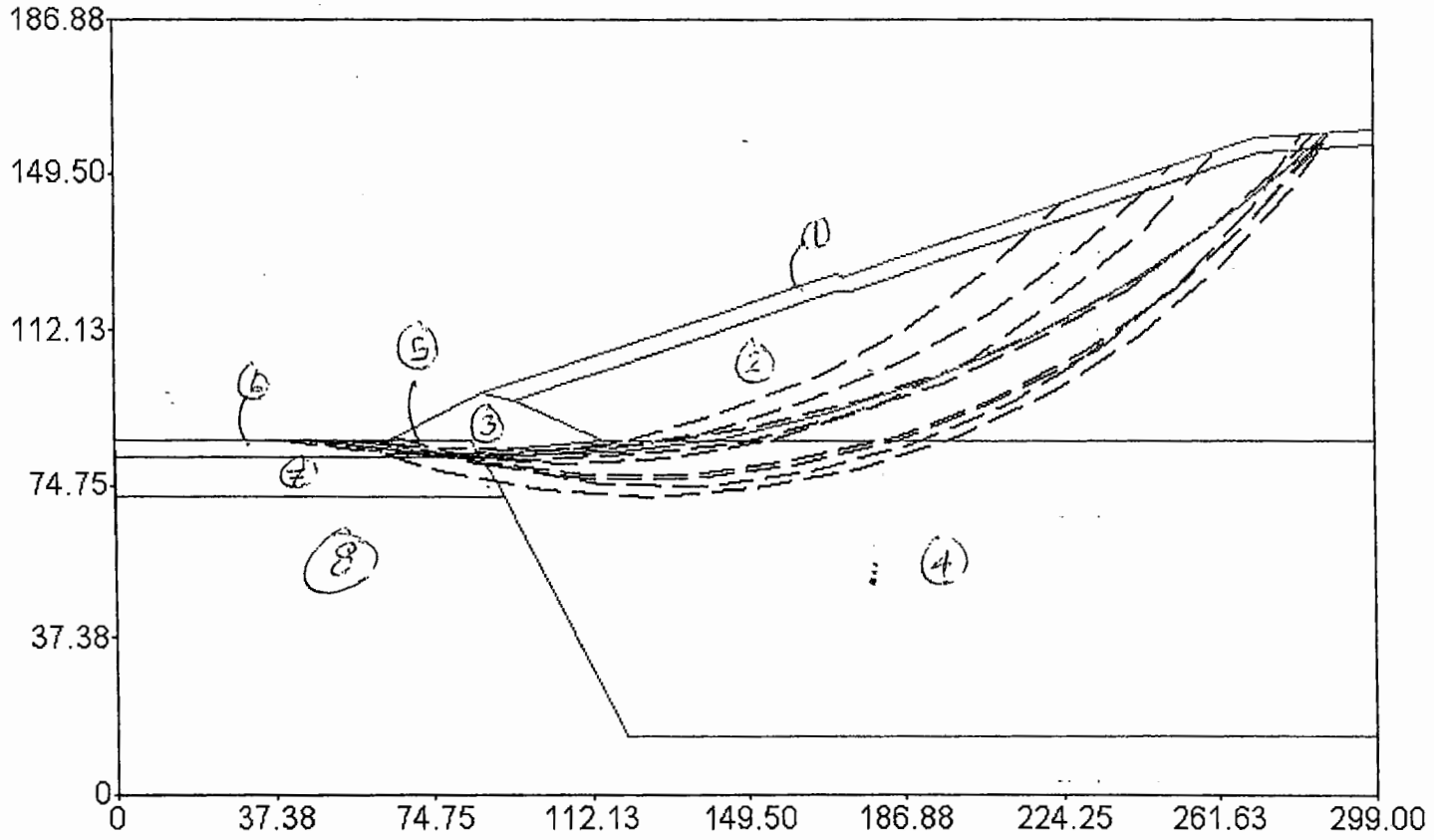

Safety Factors

0.98
0.98
1.00
1.01
1.02
1.02
1.03
1.05
1.07
1.07

Final Cover Slope Stability for section with 5 feet of surface soil.

Surface soil at C = 500 (Recompacted, with additives)

Waste at 115 PCF weight, C = 550 PSF (cohesion)

	Moist Unit Weight	Saturated Unit Weight	Isotropic Strength Intercept	Isotropic Strength Angle
1	120.00	120.00	0.00	35.00
2	115.00	115.00	550.00	27.00
3	120.00	120.00	1000.00	35.00
4	115.00	115.00	550.00	27.00
5	120.00	120.00	500.00	35.00
6	120.00	120.00	0.00	35.00
7	120.00	120.00	1440.00	35.00
8	120.00	120.00	2880.00	35.00
9	120.00	120.00	2160.00	35.00
10	120.00	120.00	4320.00	35.00

Pseudo-Static loading (0.42 g) for 5-ft thick surface soil layer

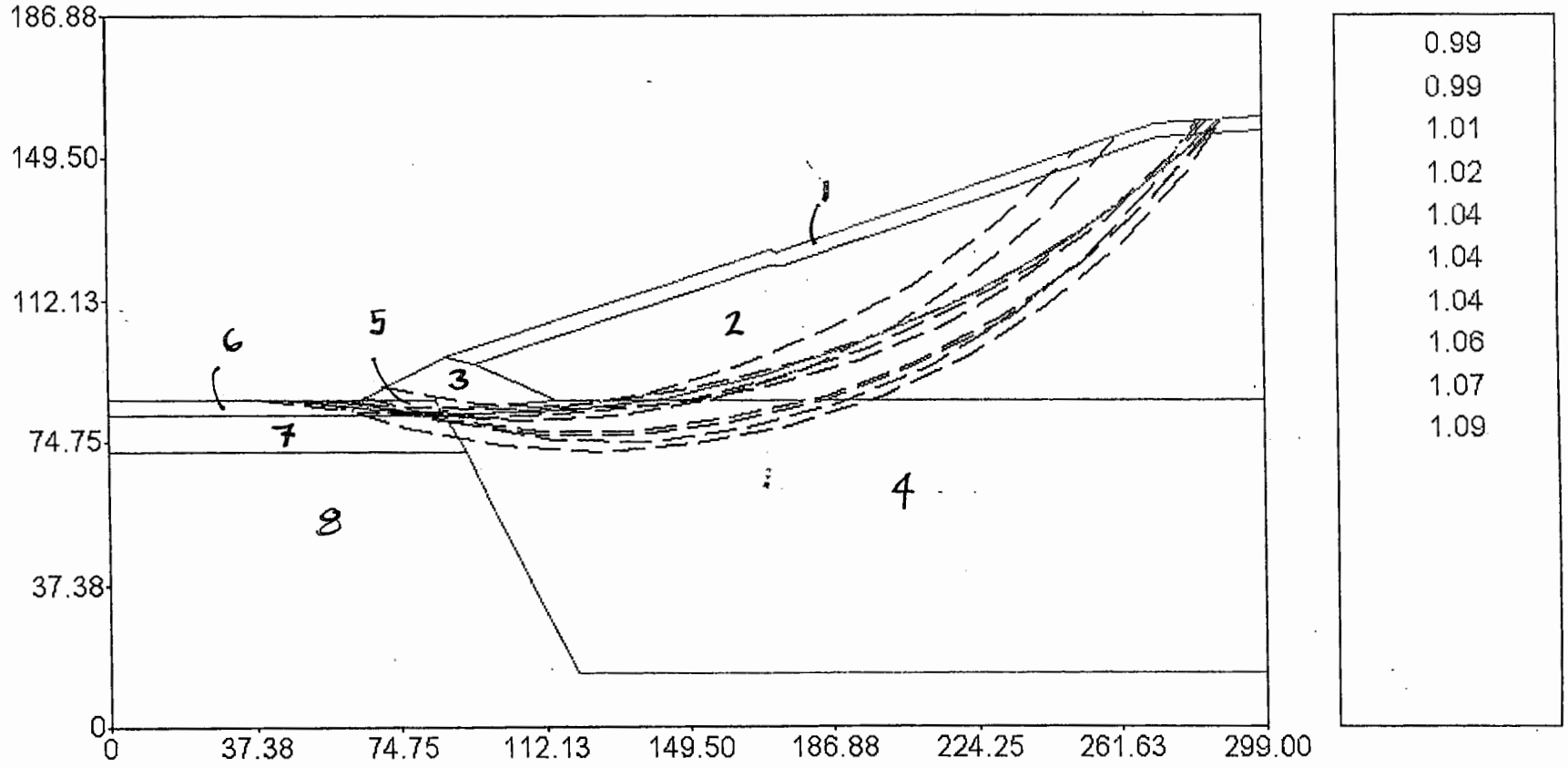

Safety Factors

0.99
0.99
1.01
1.02
1.04
1.04
1.04
1.06
1.07
1.09

Final Cover Slope Stability for section with 5 feet of surface soil

Surface soil at C = 250 PSF (recompacted, with amendment)

Waste at C = 600 PSF

	Moist Unit Weight	Saturated Unit Weight	Isotropic Strength Intercept	Isotropic Strength Angle
1	120.00	120.00	0.00	35.00
2	115.00	115.00	600.00	27.00
3	120.00	120.00	1000.00	35.00
4	115.00	115.00	600.00	27.00
5	120.00	120.00	250.00	35.00
6	120.00	120.00	0.00	35.00
7	120.00	120.00	1440.00	35.00
8	120.00	120.00	2880.00	35.00
9	120.00	120.00	2160.00	35.00
10	120.00	120.00	4320.00	35.00

Pseudo-Static loading (0.42 g) for 5-ft thick surface soil layer

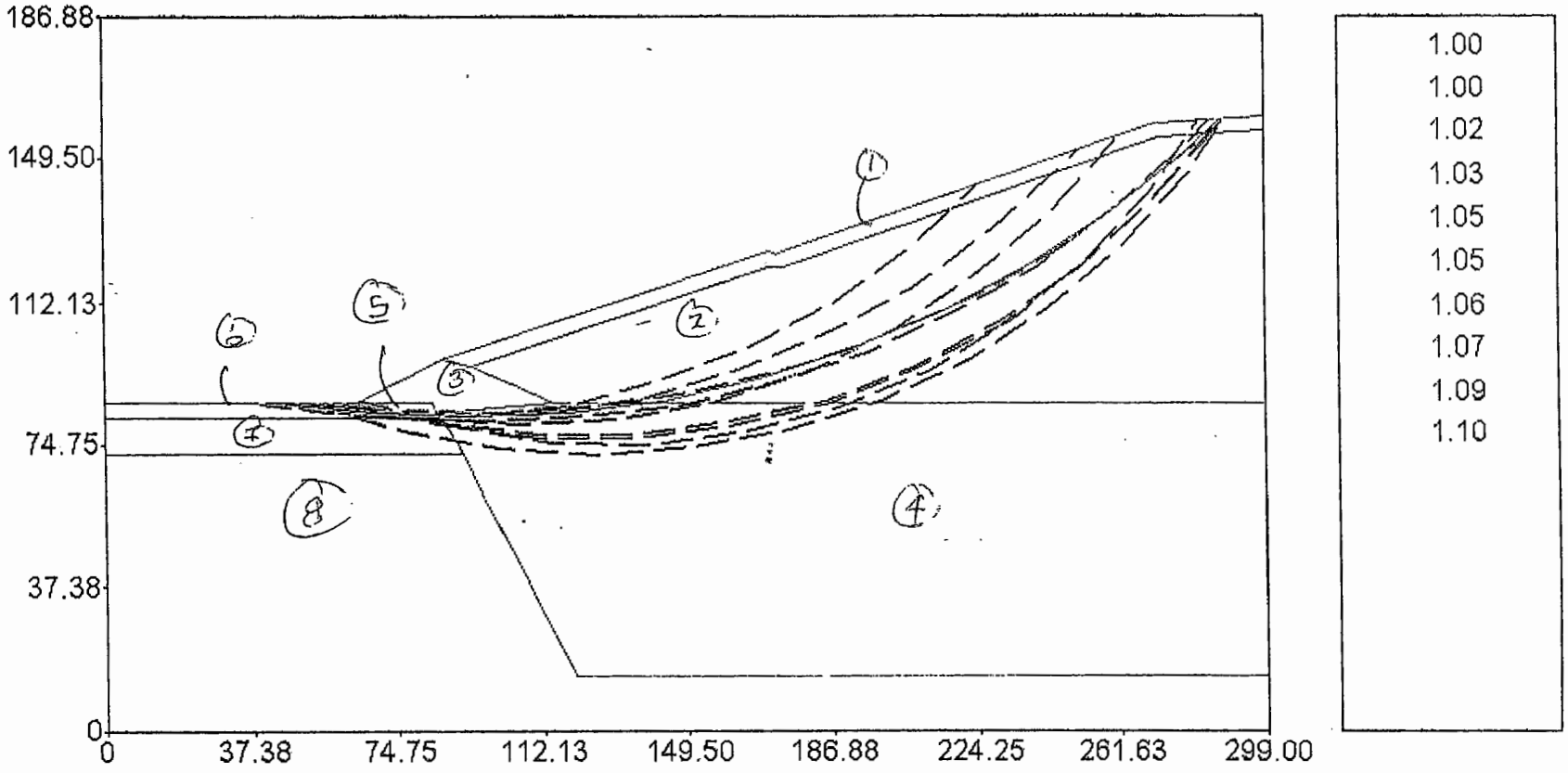

Safety Factors

1.00
1.00
1.02
1.03
1.05
1.05
1.06
1.07
1.09
1.10

Final Cover Slope Stability for section with 5 feet of surface soil

Surface soil at C = 500 PSF (recompacted, with amendment)

Waste at C = 600 PSF

	Moist Unit Weight	Saturated Unit Weight	Isotrop Strengt. Intercept	topic ength Angle	F
1	120.00	120.00	0.00	35.00	
2	115.00	115.00	600.00	27.00	
3	120.00	120.00	1000.00	35.00	
4	115.00	115.00	600.00	27.00	
5	120.00	120.00	500.00	35.00	
6	120.00	120.00	0.00	35.00	
7	120.00	120.00	1440.00	35.00	
8	120.00	120.00	2880.00	35.00	
9	120.00	120.00	2160.00	35.00	
10	120.00	120.00	4320.00	35.00	

Pseudo-Static loading (0.42 g) for 5-ft thick surface soil layer

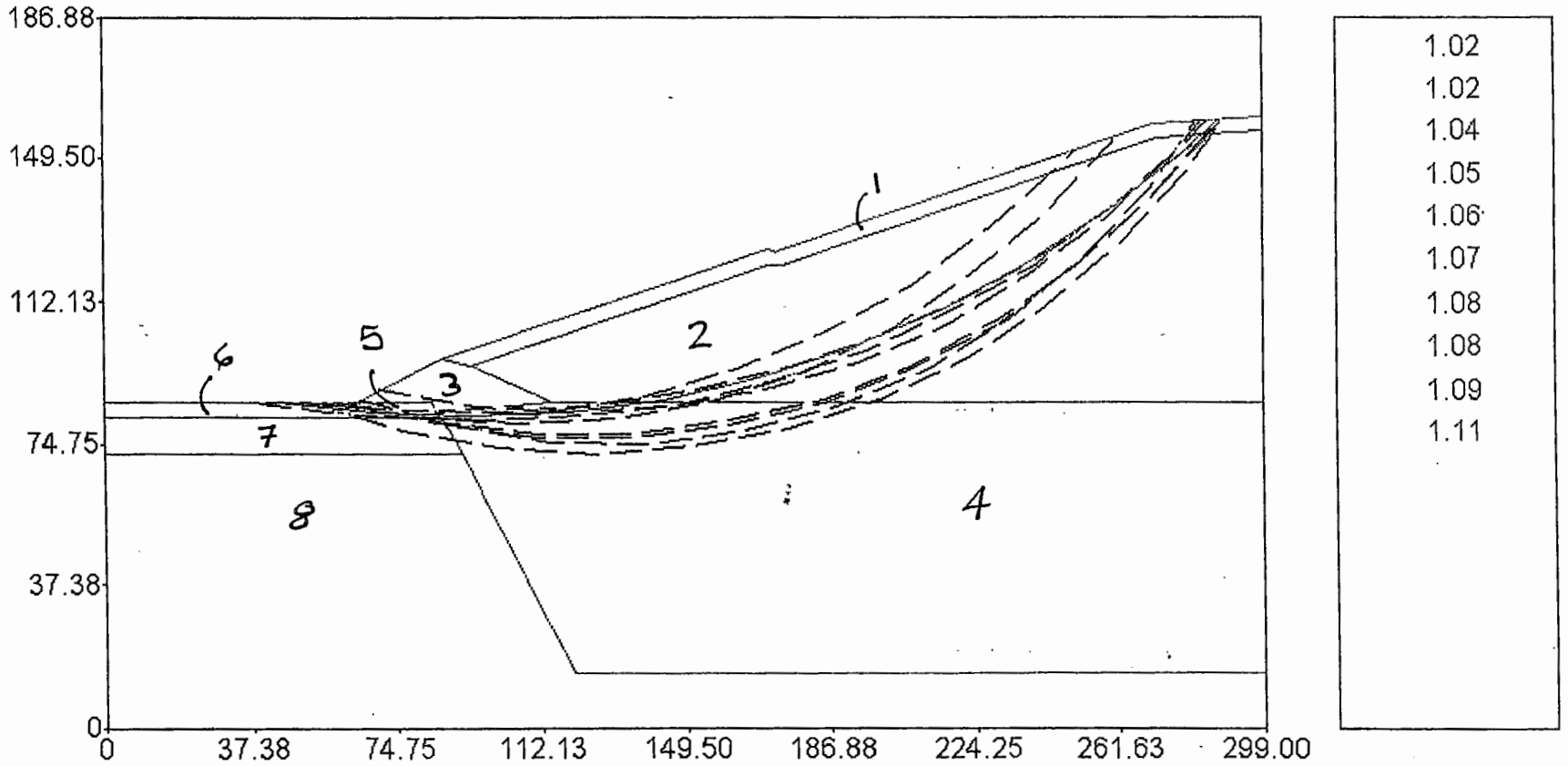

Safety Factors

1.02
1.02
1.04
1.05
1.06
1.07
1.08
1.08
1.09
1.11

Final Cover Slope Stability for section with 5 feet of surface soil.

Surface soil at C = 250 PSF (Recompacted, no additives)

Upper waste at 100 PCF weight, C = 500 PSF (cohesion)

Lower waste at 115 PCF weight, C = 500 PSF (cohesion

	Moist Unit Weight	Saturated Unit Weight	Isotropic Strength Intercept	Anisotropic Strength Angle
1	120.00	120.00	0.00	35.00
2	100.00	100.00	500.00	27.00
3	120.00	120.00	1000.00	35.00
4	115.00	115.00	500.00	27.00
5	120.00	120.00	250.00	35.00
6	120.00	120.00	0.00	35.00
7	120.00	120.00	1440.00	35.00
8	120.00	120.00	2880.00	35.00
9	120.00	120.00	2160.00	35.00
10	120.00	120.00	4320.00	35.00

Pseudo-Static loading (0.42 g) for 5-ft thick surface soil layer

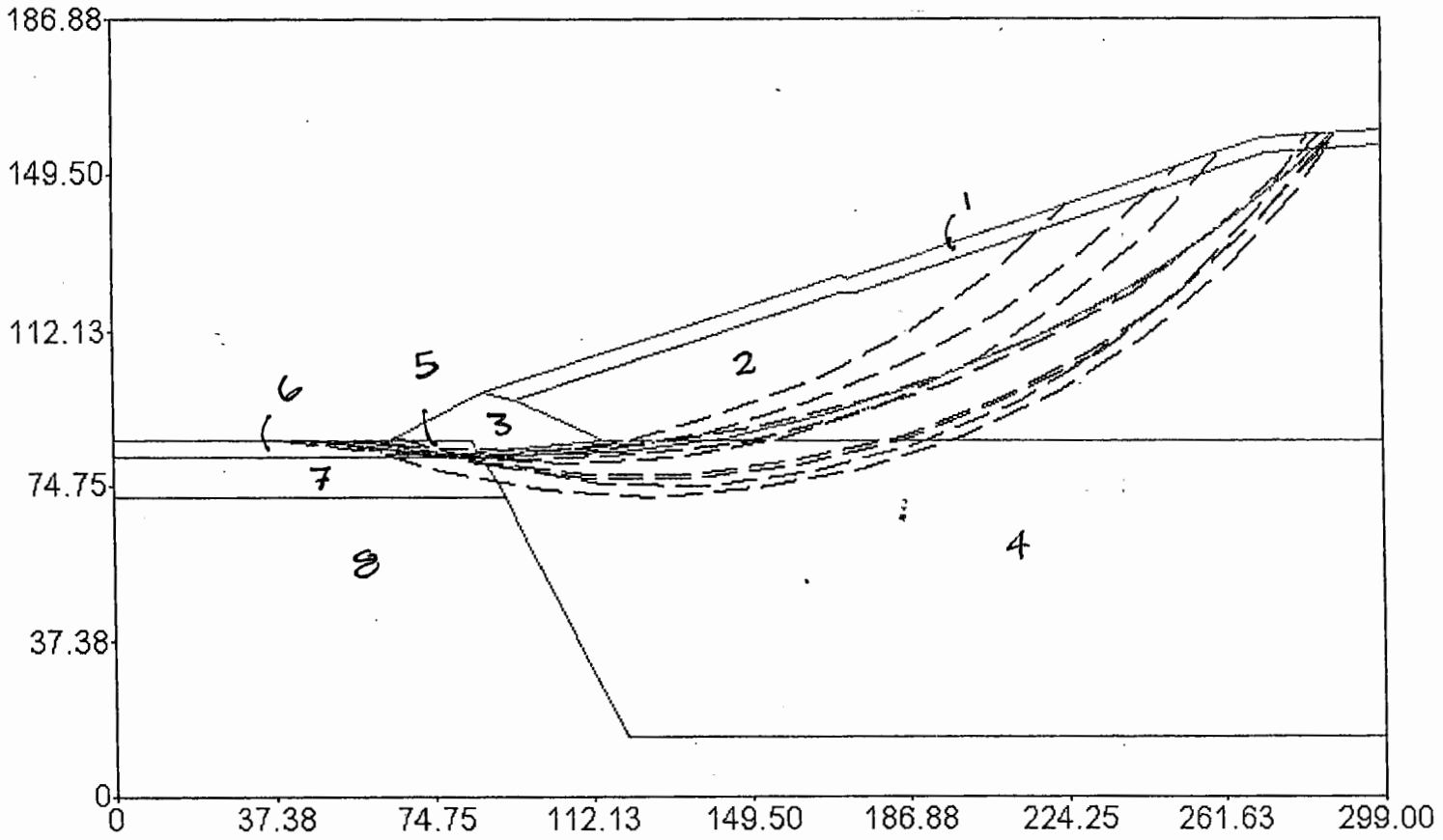

Safety Factors

0.99
0.99
1.01
1.03
1.04
1.04
1.04
1.07
1.08
1.10

	Moist Unit Weight	Saturated Unit Weight	Isotropic Strength Intercept	Isotropic Strength Angle
1	120.00	120.00	0.00	35.00
2	100.00	100.00	550.00	27.00
3	120.00	120.00	1000.00	35.00
4	115.00	115.00	550.00	27.00
5	120.00	120.00	250.00	35.00
6	120.00	120.00	0.00	35.00
7	120.00	120.00	1440.00	35.00
8	120.00	120.00	2880.00	35.00
9	120.00	120.00	2160.00	35.00
10	120.00	120.00	4320.00	35.00

Final Cover Slope Stability for section with 5 feet of surface soil.

Surface soil at C = 250 PSF (Recompacted, no additives)

Upper waste at 100 PCF weight, C = 550 PSF (cohesion)

Lower waste at 115 PCF weight, C = 550 PSF (cohesion

Pseudo-Static loading (0.42 g) for 5-ft thick surface soil layer

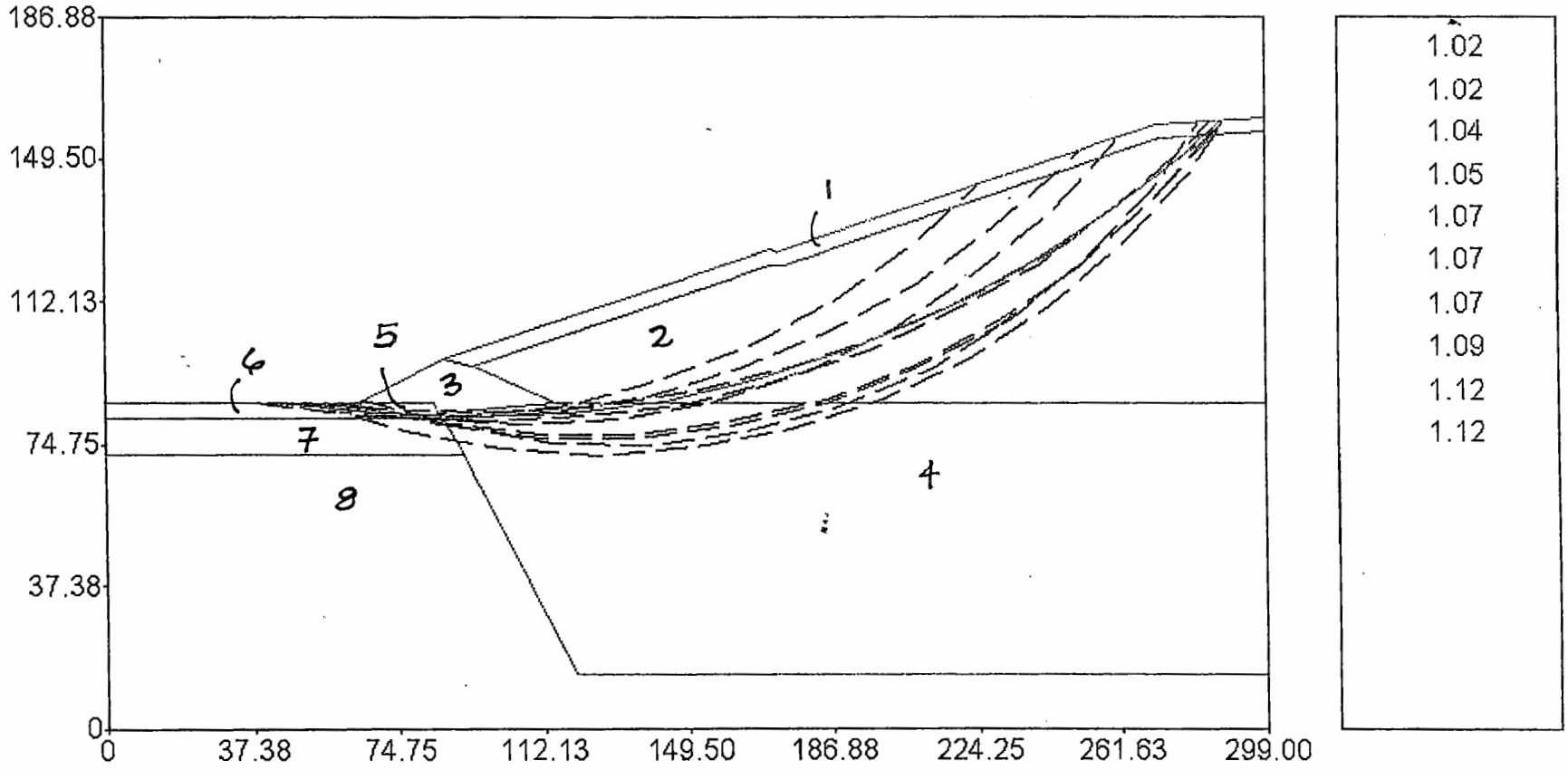

Safety Factors

1.02
1.02
1.04
1.05
1.07
1.07
1.07
1.09
1.12
1.12

5 FEET SURFACE SOIL

FINAL RUN

Surface soil $c = 250$ psf

Waste $\gamma = 100$ pcf

$c = 550$ psf

Profile.out
** PCSTABL6 **

by
Purdue University

modified by
Peter J. Bosscher
University of Wisconsin-Madison

--Slope Stability Analysis--
Simplified Janbu, Simplified Bishop
or Spencer's Method of Slices

PROBLEM DESCRIPTION Pseudo-Static loading (0.42 g) for 5-ft thick surface soil layer

BOUNDARY COORDINATES

8 Top Boundaries
29 Total Boundaries

Boundary No.	X-Left (ft)	Y-Left (ft)	X-Right (ft)	Y-Right (ft)	Soil Type Below Bnd
1	0.00	86.00	65.00	86.00	6
2	65.00	86.00	87.00	97.00	3
3	87.00	97.00	171.00	126.00	1
4	171.00	126.00	172.00	126.00	1
5	172.00	126.00	173.50	125.00	1
6	173.50	125.00	175.00	126.00	1
7	175.00	126.00	271.00	158.00	1
8	271.00	158.00	299.00	160.00	1
9	87.00	97.00	95.00	95.50	3
10	95.00	95.50	171.00	122.00	2
11	171.00	122.00	172.00	122.00	2
12	172.00	122.00	173.50	121.00	2
13	173.50	121.00	175.00	122.00	2
14	175.00	122.00	272.00	154.50	2
15	272.00	154.50	299.00	156.00	2
16	95.00	95.50	116.00	86.00	3
17	116.00	86.00	299.00	86.00	4
18	65.00	86.00	85.00	86.00	5
19	85.00	86.00	86.00	83.00	5
20	86.00	83.00	116.00	86.00	4
21	86.00	83.00	87.00	81.00	5
22	87.00	81.00	92.00	72.00	7
23	92.00	72.00	97.00	62.00	8
24	97.00	62.00	120.00	14.00	8
25	120.00	14.00	299.00	14.00	8

26	65.00	86.00	70.00	81.00	6
27	70.00	81.00	87.00	81.00	7
28	0.00	81.00	70.00	81.00	7
29	0.00	72.00	92.00	72.00	8

ISOTROPIC SOIL PARAMETERS

10 Type(s) of Soil

Soil Type No.	Total Unit Wt. (pcf)	Saturated Unit Wt. (pcf)	Cohesion Intercept (psf)	Friction Angle (deg)	Pore Pressure Param.	Pressure Constant (psf)	Piez. Surface No.
1	120.0	120.0	0.0	35.0	0.00	0.0	0
2	100.0	100.0	550.0	27.0	0.00	0.0	0
3	120.0	120.0	1000.0	35.0	0.00	0.0	0
4	115.0	115.0	550.0	27.0	0.00	0.0	0
5	120.0	120.0	250.0	35.0	0.00	0.0	0
6	120.0	120.0	0.0	35.0	0.00	0.0	0
7	120.0	120.0	1440.0	35.0	0.00	0.0	0
8	120.0	120.0	2880.0	35.0	0.00	0.0	0
9	120.0	120.0	2160.0	35.0	0.00	0.0	0
10	120.0	120.0	4320.0	35.0	0.00	0.0	0

A Horizontal Earthquake Loading Coefficient
Of0.420 Has Been Assigned

A Vertical Earthquake Loading Coefficient
Of0.000 Has Been Assigned

Cavitation Pressure = 0.0 psf

A Critical Failure Surface Searching Method, Using A Random Technique For Generating Circular Surfaces, Has Been Specified.

100 Trial Surfaces Have Been Generated.

10 Surfaces Initiate From Each Of 10 Points Equally Spaced Along The Ground Surface Between X = 40.00 ft.
and X = 80.00 ft.

Each Surface Terminates Between X = 150.00 ft.
and X = 290.00 ft.

Unless Further Limitations Were Imposed, The Minimum Elevation At Which A Surface Extends Is Y = 70.00 ft.

25.00 ft. Line Segments Define Each Trial Failure Surface.

Following Are Displayed The Ten Most Critical Of The Trial Failure Surfaces Examined. They Are Ordered - Most Critical First.

* * Safety Factors Are Calculated By The Modified Bishop Method * *

Failure Surface Specified By 12 Coordinate Points

Point No.	X-Surf (ft)	Y-Surf (ft)
1	44.44	86.00
2	69.25	82.86
3	94.23	81.89
4	119.20	83.11
5	143.97	86.50
6	168.34	92.04
7	192.15	99.69
8	215.19	109.39
9	237.30	121.06
10	258.30	134.62
11	278.04	149.96
12	288.02	159.22

Circle Center At X = 92.8 ; Y = 368.0 and Radius, 286.1

*** 1.018 ***

Failure Surface Specified By 12 Coordinate Points

Point No.	X-Surf (ft)	Y-Surf (ft)
1	48.89	86.00
2	73.62	82.34
3	98.59	81.06
4	123.56	82.17
5	148.32	85.65
6	172.63	91.47
7	196.28	99.59
8	219.04	109.93
9	240.71	122.39
10	261.10	136.86
11	280.02	153.20
12	285.59	159.04

Circle Center At X = 99.5 ; Y = 342.9 and Radius, 261.9

*** 1.020 ***

Failure Surface Specified By 12 Coordinate Points

Point No.	X-Surf (ft)	Y-Surf (ft)
1	53.33	86.00
2	78.22	83.64
3	103.22	83.43
4	128.15	85.35
5	152.82	89.41
6	177.05	95.56
7	200.66	103.76
8	223.49	113.96
9	245.36	126.07
10	266.11	140.02
11	285.59	155.69
12	289.38	159.31

Circle Center At X = 93.2 ; Y = 374.9 and Radius, 291.6

*** 1.039 ***

Failure Surface Specified By 12 Coordinate Points

Point No.	X-Surf (ft)	Y-Surf (ft)
1	62.22	86.00
2	86.57	80.31
3	111.41	77.54
4	136.41	77.75
5	161.21	80.92
6	185.46	87.02
7	208.81	95.95
8	230.93	107.58
9	251.52	121.77
10	270.28	138.30
11	286.94	156.93
12	288.56	159.25

Circle Center At X = 122.2 ; Y = 287.5 and Radius, 210.2

*** 1.054 ***

Failure Surface Specified By 11 Coordinate Points

Point No.	X-Surf (ft)	Y-Surf (ft)
1	57.78	86.00
2	82.35	81.39
3	107.31	79.92
4	132.25	81.62
5	156.78	86.45
6	180.50	94.35

7	203.03	105.17
8	224.02	118.76
9	243.12	134.89
10	260.03	153.30
11	261.00	154.67

Circle Center At X = 106.4 ; Y = 277.4 and Radius, 197.5

*** 1.065 ***

Failure Surface Specified By 12 Coordinate Points

Point No.	X-Surf (ft)	Y-Surf (ft)
1	62.22	86.00
2	86.46	79.87
3	111.27	76.77
4	136.27	76.73
5	161.08	79.76
6	185.34	85.82
7	208.67	94.81
8	230.71	106.59
9	251.15	120.99
10	269.66	137.80
11	285.97	156.74
12	287.59	159.19

Circle Center At X = 124.1 ; Y = 279.6 and Radius, 203.2

*** 1.068 ***

Failure Surface Specified By 11 Coordinate Points

Point No.	X-Surf (ft)	Y-Surf (ft)
1	40.00	86.00
2	64.75	82.45
3	89.73	81.58
4	114.67	83.39
5	139.26	87.85
6	163.24	94.93
7	186.32	104.53
8	208.24	116.55
9	228.75	130.85
10	247.61	147.27
11	251.54	151.51

Circle Center At X = 85.4 ; Y = 314.6 and Radius, 233.1

*** 1.071 ***

Failure Surface Specified By 11 Coordinate Points

Point No.	X-Surf (ft)	Y-Surf (ft)
1	66.67	86.83
2	90.58	79.55
3	115.28	75.67
4	140.28	75.25
5	165.09	78.32
6	189.23	84.82
7	212.23	94.60
8	233.65	107.50
9	253.07	123.24
10	270.11	141.54
11	282.18	158.80

Circle Center At X = 130.7 ; Y = 254.3 and Radius, 179.3

*** 1.094 ***

Failure Surface Specified By 9 Coordinate Points

Point No.	X-Surf (ft)	Y-Surf (ft)
1	44.44	86.00
2	69.23	82.74
3	94.23	82.62
4	119.05	85.65
5	143.28	91.78
6	166.56	100.90
7	188.50	112.89
8	208.76	127.54
9	224.89	142.63

Circle Center At X = 82.7 ; Y = 280.6 and Radius, 198.3

*** 1.115 ***

Failure Surface Specified By 12 Coordinate Points

Point No.	X-Surf (ft)	Y-Surf (ft)
1	53.33	86.00
2	77.13	78.33
3	101.70	73.72
4	126.66	72.24
5	151.60	73.92
6	176.13	78.73
7	199.86	86.59
8	222.42	97.38

9	243.43	110.92
10	262.57	127.01
11	279.53	145.37
12	289.46	159.32

Circle Center At X = 125.9 ; Y = 270.2 and Radius, 198.0

*** 1.119 ***

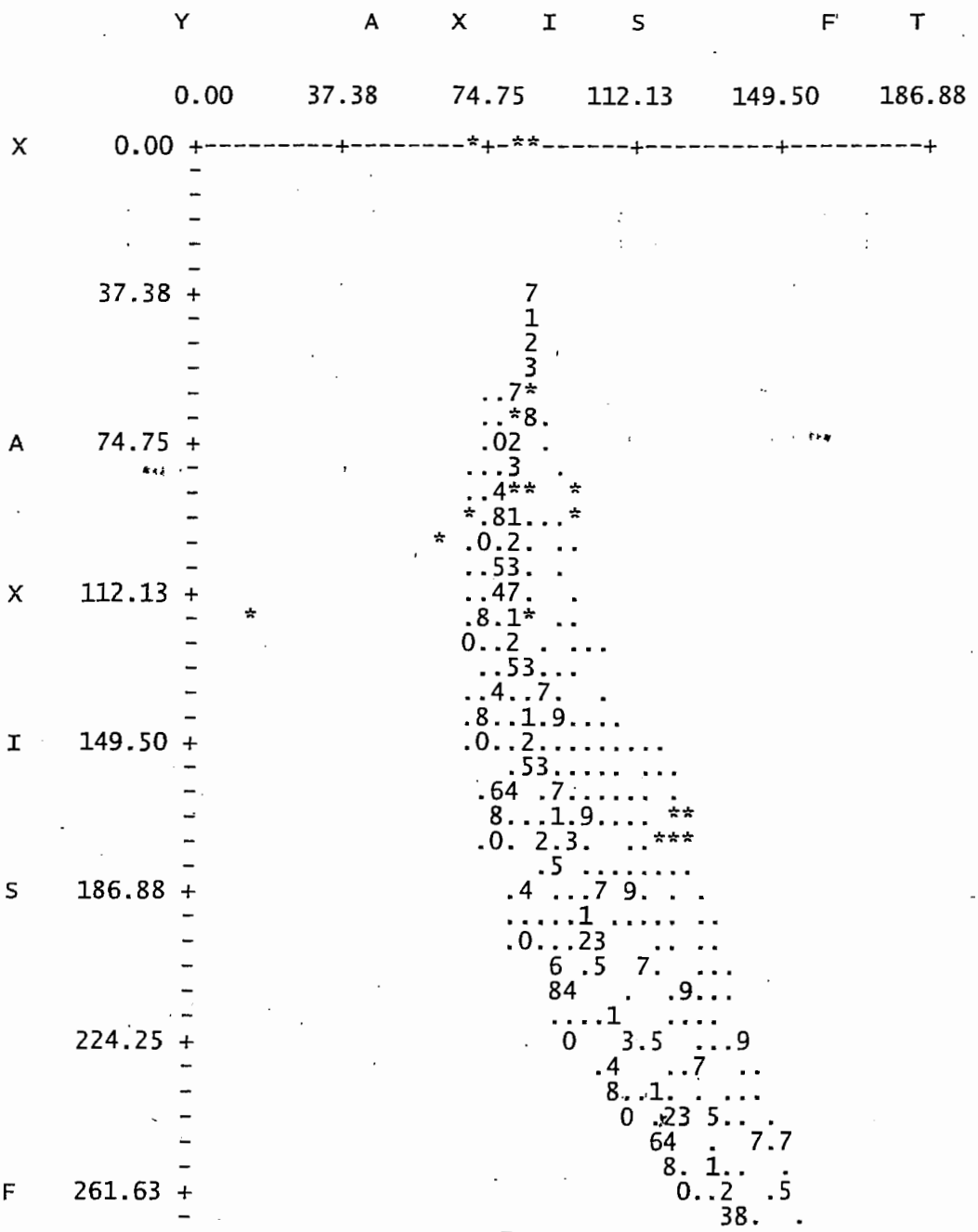

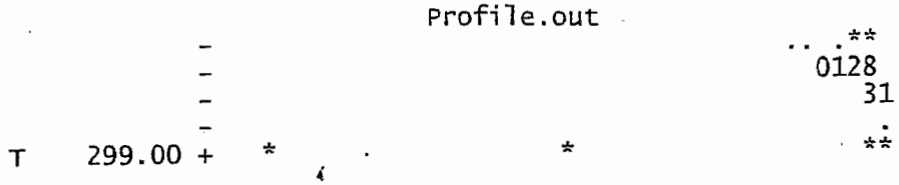
T
299.00

Final Cover Slope Stability for section with 10 feet of surface soil

Surface soil at C = 0 PSF (no recompaction)

Waste at C = 500 PSF

	Moist Unit Weight	Saturated Unit Weight	Isotro Streng.. Intercept	opic ngth Angle
1	120.00	120.00	0.00	35.00
2	115.00	115.00	500.00	27.00
3	120.00	120.00	1000.00	35.00
4	115.00	115.00	500.00	27.00
5	120.00	120.00	0.00	35.00
6	120.00	120.00	0.00	35.00
7	120.00	120.00	1440.00	35.00
8	120.00	120.00	2880.00	35.00
9	120.00	120.00	2160.00	35.00
10	120.00	120.00	4320.00	35.00

Pseudo-Static loading (0.42 g horiz accel) for 10 ft thick improved surface soil layer

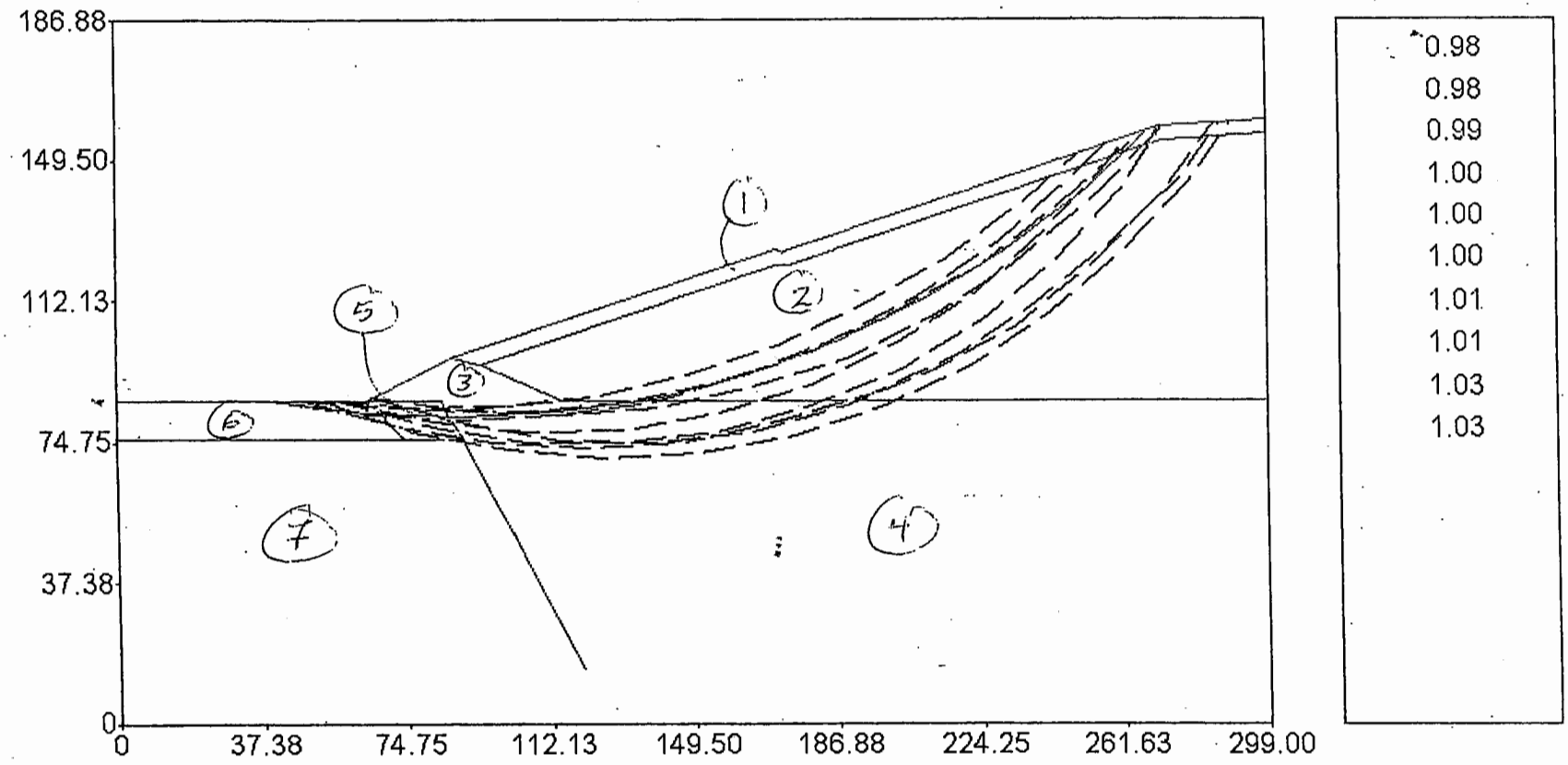

Safety Factors

0.98
0.98
0.99
1.00
1.00
1.00
1.01
1.01
1.03
1.03

Final Cover Slope Stability for section with 10 feet of surface soil

Surface soil at C = 250 PSF (recompacted, no amendment)

Waste at C = 500 PSF

	Moist Unit Weight	Saturated Unit Weight	Isotropic Strength Intercept	Isotropic Strength Angle
1	120.00	120.00	0.00	35.00
2	115.00	115.00	500.00	27.00
3	120.00	120.00	1000.00	35.00
4	115.00	115.00	500.00	27.00
5	120.00	120.00	250.00	35.00
6	120.00	120.00	0.00	35.00
7	120.00	120.00	1440.00	35.00
8	120.00	120.00	2880.00	35.00
9	120.00	120.00	2160.00	35.00
10	120.00	120.00	4320.00	35.00

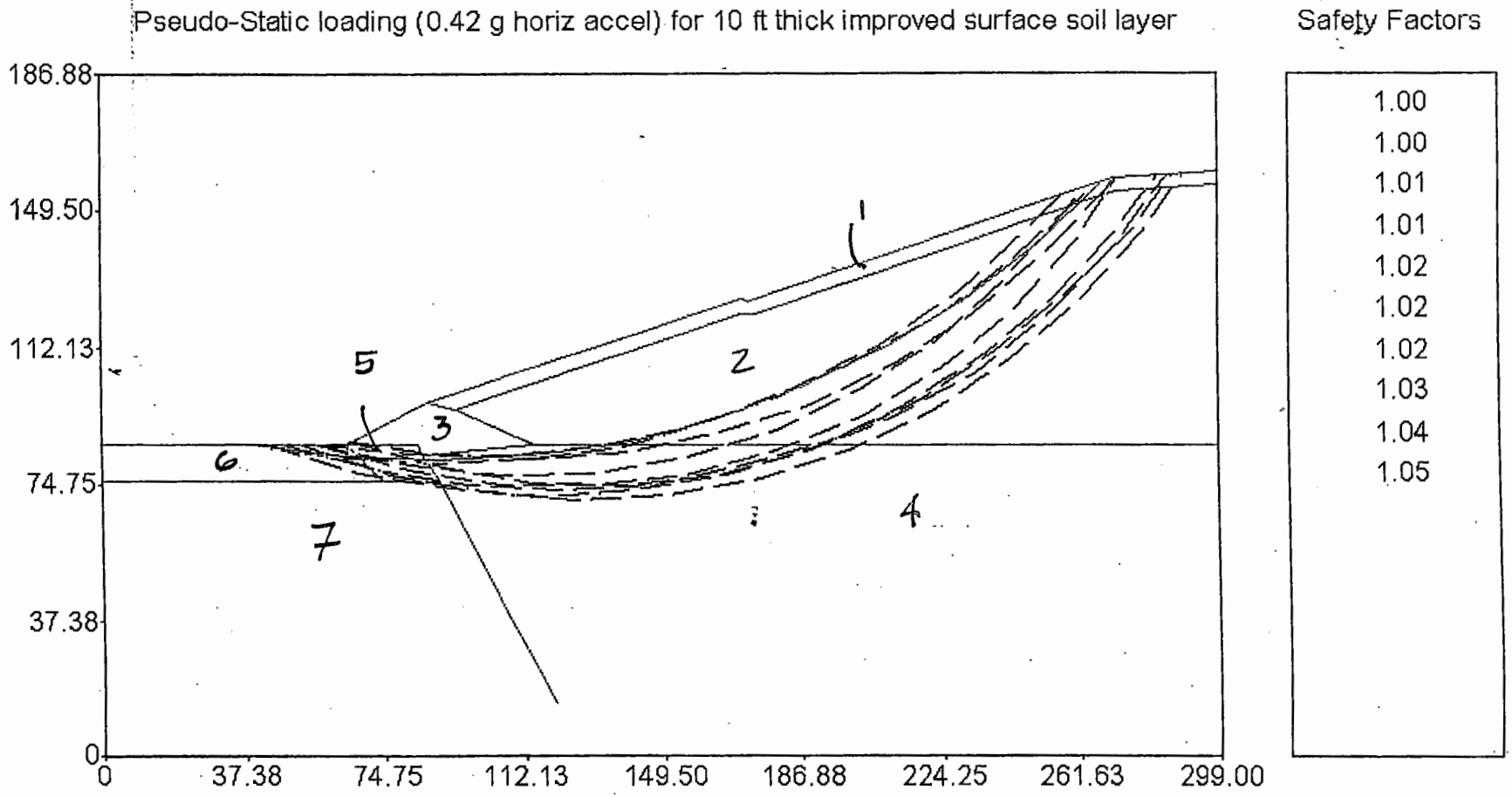

Final Cover Slope Stability for section with 10 feet of surface soil

Surface soil at C = 250 PSF (recompacted, no amendment)

Waste at C = 550 PSF

	Moist Unit Weight	Saturated Unit Weight	Isotropic Strength Intercept	Isotropic Strength Angle
1	120.00	120.00	0.00	35.00
2	115.00	115.00	550.00	27.00
3	120.00	120.00	1000.00	35.00
4	115.00	115.00	550.00	27.00
5	120.00	120.00	250.00	35.00
6	120.00	120.00	0.00	35.00
7	120.00	120.00	1440.00	35.00
8	120.00	120.00	2880.00	35.00
9	120.00	120.00	2160.00	35.00
10	120.00	120.00	4320.00	35.00

Pseudo-Static loading (0.42 g horiz accel) for 10 ft thick improved surface soil layer

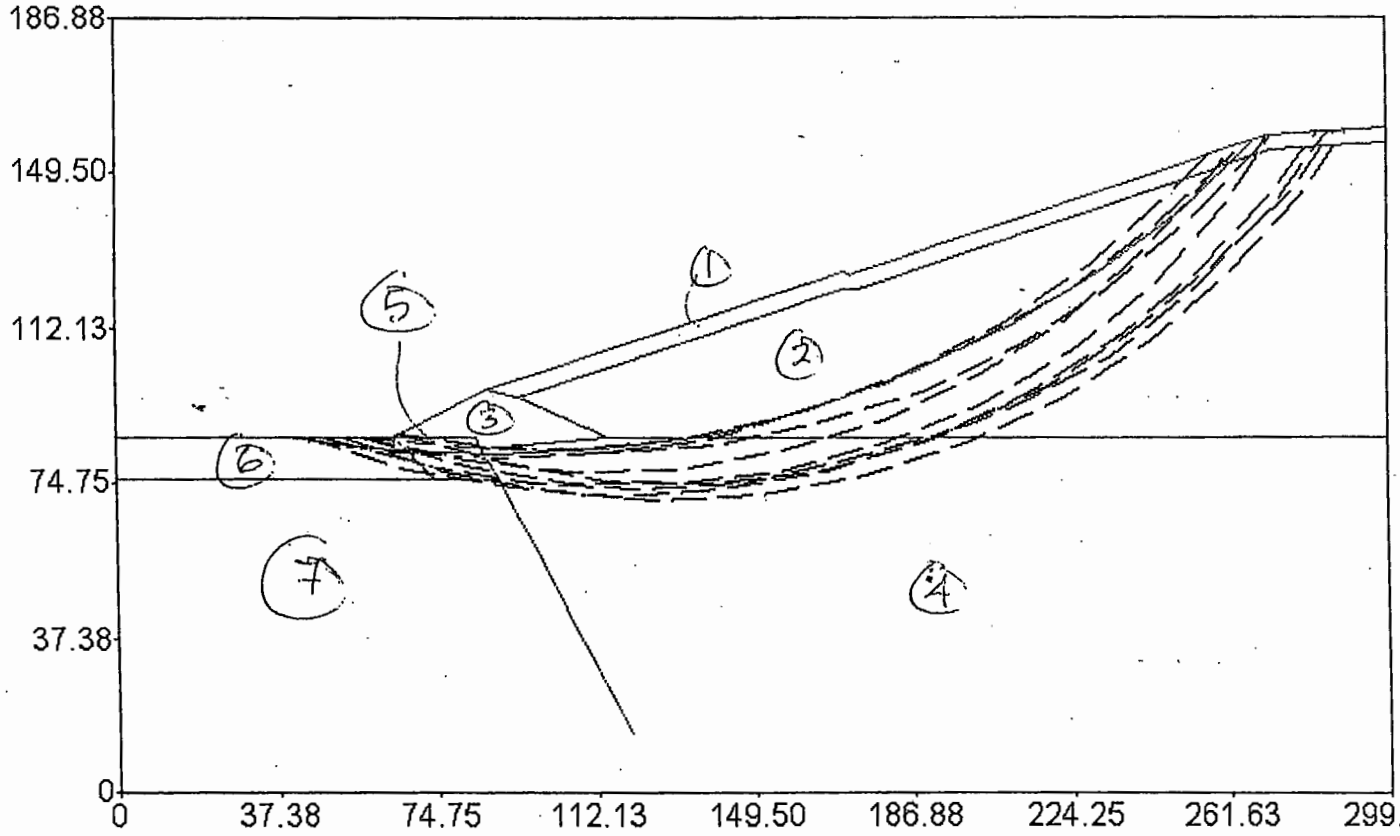

Safety Factors

1.02
1.03
1.03
1.04
1.04
1.04
1.04
1.05
1.06
1.07

Final Cover Slope Stability for section with 10 feet of surface soil

Surface soil at C = 250 PSF (recompacted, no amendment)

Waste at C = 600 PSF

	Moist Unit Weight	Saturated Unit Weight	Isotropic Strength Intercept	Isotropic Strength Angle
1	120.00	120.00	0.00	35.00
2	115.00	115.00	600.00	27.00
3	120.00	120.00	1000.00	35.00
4	115.00	115.00	600.00	27.00
5	120.00	120.00	250.00	35.00
6	120.00	120.00	0.00	35.00
7	120.00	120.00	1440.00	35.00
8	120.00	120.00	2880.00	35.00
9	120.00	120.00	2160.00	35.00
10	120.00	120.00	4320.00	35.00

Pseudo-Static loading (0.42 g horiz accel) for 10 ft thick improved surface soil layer

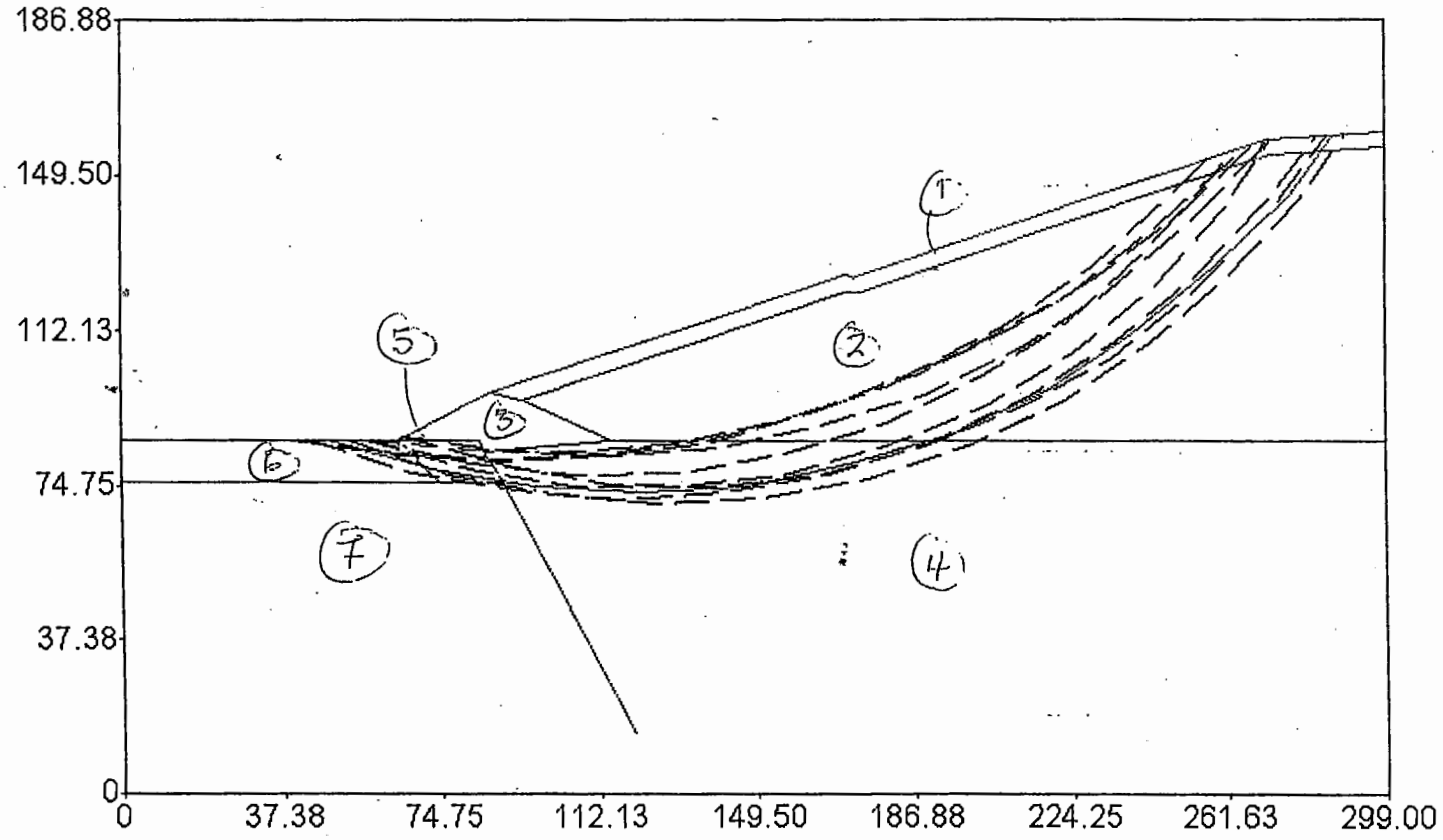

Safety Factors

1.05
1.05
1.06
1.06
1.06
1.06
1.07
1.07
1.08
1.09

Final Cover Slope Stability for section with 10 feet of surface soil.

Surface soil at C = 250 (Recompacted, no additives)

Upper waste at 100 PCF weight, C = 550 PSF (cohesion)

Lower waste at 115 PCF weight, C = 550 PSF (cohesion

	Moist Unit Weight	Saturated Unit Weight	Isotr... Stre... Intercept	...tropic ...rength Angle
1	120.00	120.00	0.00	35.00
2	100.00	100.00	550.00	27.00
3	120.00	120.00	1000.00	35.00
4	115.00	115.00	550.00	27.00
5	120.00	120.00	250.00	35.00
6	120.00	120.00	0.00	35.00
7	120.00	120.00	1440.00	35.00
8	120.00	120.00	2880.00	35.00
9	120.00	120.00	2160.00	27.00
10	120.00	120.00	4320.00	35.00

Pseudo-static loading (0.42 g horiz accel)

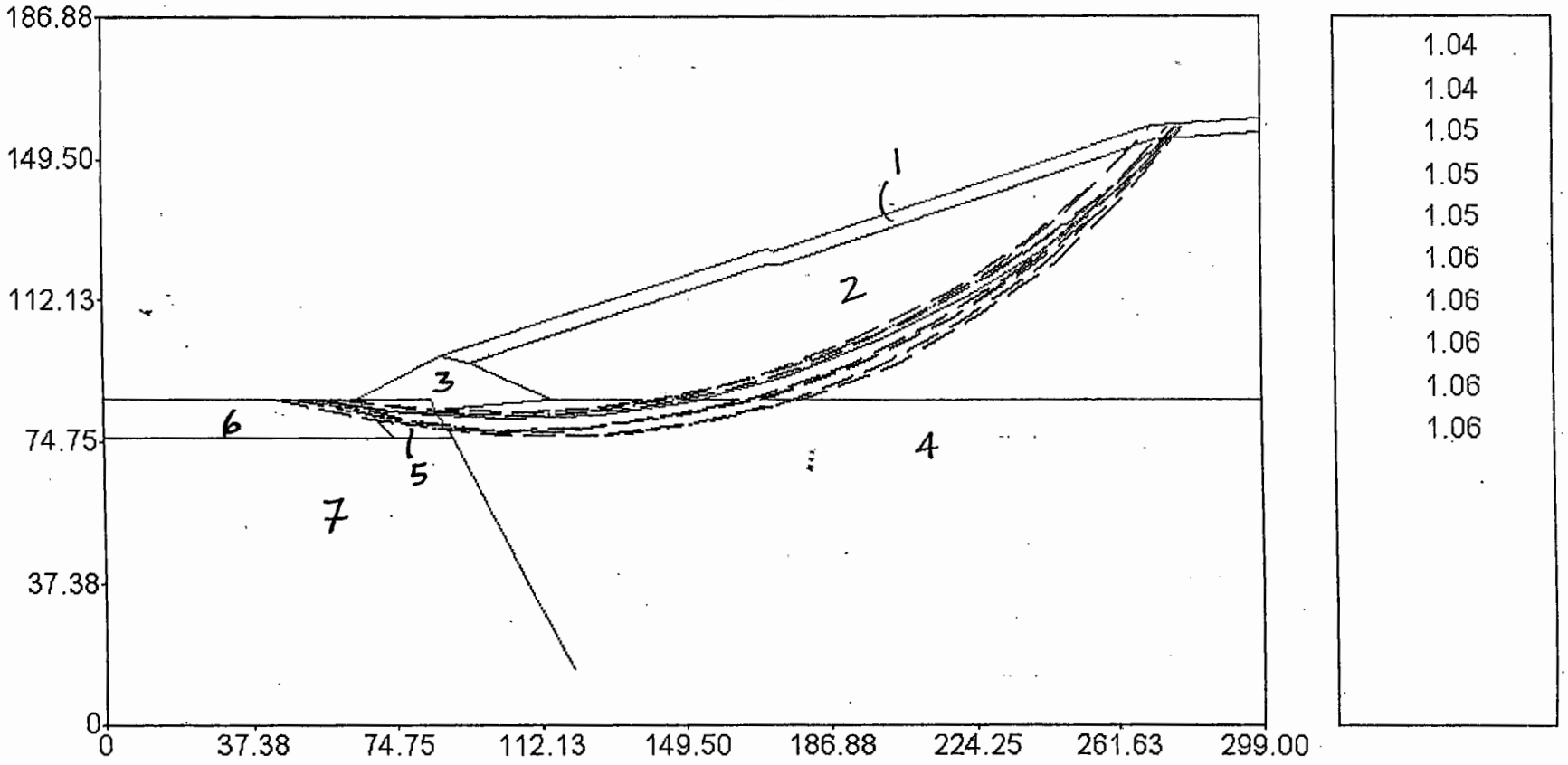

Safety Factors

1.04
1.04
1.05
1.05
1.05
1.06
1.06
1.06
1.06
1.06

10 FEET SURFACE SOIL

FINAL RUN

Surface soil C=250psf

Waste γ=100pcf

C= 550psf

Profile.out
** PCSTABL6 **

by
Purdue University

modified by
Peter J. Bosscher
University of Wisconsin-Madison

--Slope Stability Analysis--
Simplified Janbu, Simplified Bishop
or Spencer's Method of Slices

PROBLEM DESCRIPTION Pseudo-static loading (0.42 g horiz acce
l)

BOUNDARY COORDINATES

8 Top Boundaries
24 Total Boundaries

Boundary No.	X-Left (ft)	Y-Left (ft)	X-Right (ft)	Y-Right (ft)	Soil Type Below Bnd
1	0.00	86.00	65.00	86.00	6
2	65.00	86.00	87.00	97.00	3
3	87.00	97.00	171.00	126.00	1
4	171.00	126.00	172.00	126.00	1
5	172.00	126.00	173.50	125.00	1
6	173.50	125.00	175.00	126.00	1
7	175.00	126.00	271.00	158.00	1
8	271.00	158.00	299.00	160.00	1
9	87.00	97.00	95.00	95.50	3
10	95.00	95.50	171.00	122.00	2
11	171.00	122.00	172.00	122.00	2
12	172.00	122.00	173.50	121.00	2
13	173.50	121.00	175.00	122.00	2
14	175.00	122.00	272.00	154.50	2
15	272.00	154.50	299.00	156.00	2
16	95.00	95.50	116.00	86.00	3
17	116.00	86.00	299.00	86.00	4
18	65.00	86.00	85.00	86.00	5
19	85.00	86.00	86.00	83.00	5
20	86.00	83.00	116.00	86.00	4
21	86.00	83.00	90.00	76.00	5
22	90.00	76.00	120.00	14.00	7
23	65.00	86.00	75.00	76.00	7
24	0.00	76.00	90.00	76.00	7

ISOTROPIC SOIL PARAMETERS

10 Type(s) of Soil

Soil Type No.	Total Unit Wt. (pcf)	Saturated Unit Wt. (pcf)	Cohesion Intercept (psf)	Friction Angle (deg)	Pore Pressure Param.	Pressure Constant (psf)	Piez. Surface No.
1	120.0	120.0	0.0	35.0	0.00	0.0	0
2	100.0	100.0	550.0	27.0	0.00	0.0	0
3	120.0	120.0	1000.0	35.0	0.00	0.0	0
4	115.0	115.0	550.0	27.0	0.00	0.0	0
5	120.0	120.0	250.0	35.0	0.00	0.0	0
6	120.0	120.0	0.0	35.0	0.00	0.0	0
7	120.0	120.0	1440.0	35.0	0.00	0.0	0
8	120.0	120.0	2880.0	35.0	0.00	0.0	0
9	120.0	120.0	2160.0	35.0	0.00	0.0	0
10	120.0	120.0	4320.0	35.0	0.00	0.0	0

A Horizontal Earthquake Loading Coefficient
Of0.420 Has Been Assigned

A Vertical Earthquake Loading Coefficient
Of0.000 Has Been Assigned

Cavitation Pressure = 0.0 psf

A Critical Failure Surface Searching Method, Using A Random Technique For Generating Circular Surfaces, Has Been Specified.

100 Trial Surfaces Have Been Generated.

10 Surfaces Initiate From Each Of 10 Points Equally Spaced Along The Ground Surface Between X = 40.00 ft.
and X = 80.00 ft.

Each Surface Terminates Between X = 200.00 ft.
and X = 280.00 ft.

Unless Further Limitations Were Imposed, The Minimum Elevation At Which A Surface Extends Is Y = 74.00 ft.

25.00 ft. Line Segments Define Each Trial Failure Surface.

Following Are Displayed The Ten Most Critical Of The Trial Failure Surfaces Examined. They Are Ordered - Most Critical First.

* * Safety Factors Are Calculated By The Modified Bishop Method * *

Failure Surface Specified By 11 Coordinate Points

Point No.	X-Surf (ft)	Y-Surf (ft)
1	53.33	86.00
2	77.99	81.88
3	102.95	80.40
4	127.92	81.59
5	152.62	85.43
6	176.78	91.88
7	200.11	100.86
8	222.35	112.27
9	243.26	125.98
10	262.58	141.84
11	279.03	158.57

Circle Center At X = 104.3 ; Y = 315.0 and Radius, 234.6

*** 1.044 ***

Failure Surface Specified By 11 Coordinate Points

Point No.	X-Surf (ft)	Y-Surf (ft)
1	53.33	86.00
2	78.11	82.69
3	103.10	81.88
4	128.04	83.58
5	152.69	87.76
6	176.80	94.39
7	200.12	103.40
8	222.42	114.69
9	243.48	128.17
10	263.08	143.68
11	278.41	158.53

Circle Center At X = 98.7 ; Y = 331.3 and Radius, 249.4

*** 1.045 ***

Failure Surface Specified By 11 Coordinate Points

Point No.	X-Surf (ft)	Y-Surf (ft)
1	62.22	86.00
2	87.05	83.07

3	112.05	82.73
4	136.95	85.00
5	161.47	89.84
6	185.36	97.20
7	208.36	107.00
8	230.22	119.14
9	250.69	133.49
10	269.56	149.88
11	277.58	158.47

Circle Center At X = 102.8 ; Y = 322.8 and Radius, 240.3

*** 1.049 ***

Failure Surface Specified By 12 Coordinate Points

Point No.	X-Surf (ft)	Y-Surf (ft)
1	48.89	86.00
2	73.32	80.67
3	98.18	78.12
4	123.18	78.37
5	148.00	81.43
6	172.31	87.25
7	195.82	95.76
8	218.22	106.86
9	239.24	120.39
10	258.60	136.20
11	276.07	154.09
12	279.59	158.61

Circle Center At X = 108.4 ; Y = 300.4 and Radius, 222.5

*** 1.051 ***

Failure Surface Specified By 12 Coordinate Points

Point No.	X-Surf (ft)	Y-Surf (ft)
1	48.89	86.00
2	73.33	80.73
3	98.20	78.24
4	123.20	78.57
5	148.00	81.70
6	172.30	87.61
7	195.77	96.21
8	218.13	107.39
9	239.08	121.03
10	258.37	136.93
11	275.75	154.90
12	278.56	158.54

Circle Center At X = 107.8 ; Y = 299.9 and Radius, 221.9

*** 1.053 ***

Failure Surface Specified By 11 Coordinate Points

Point No.	X-Surf (ft)	Y-Surf (ft)
1	48.89	86.00
2	73.59	82.15
3	98.56	80.95
4	123.52	82.39
5	148.19	86.47
6	172.28	93.14
7	195.53	102.33
8	217.68	113.93
9	238.47	127.81
10	257.68	143.81
11	271.47	158.03

Circle Center At X = 97.4 ; Y = 316.6 and Radius, 235.6

*** 1.059 ***

Failure Surface Specified By 11 Coordinate Points

Point No.	X-Surf (ft)	Y-Surf (ft)
1	62.22	86.00
2	86.94	82.23
3	111.92	81.38
4	136.84	83.45
5	161.34	88.41
6	185.09	96.20
7	207.77	106.72
8	229.07	119.81
9	248.70	135.30
10	266.38	152.98
11	270.11	157.70

Circle Center At X = 106.7 ; Y = 295.0 and Radius, 213.7

*** 1.060 ***

Failure Surface Specified By 12 Coordinate Points

Point No.	X-Surf (ft)	Y-Surf (ft)
1	44.44	86.00

2	68.82	80.42
3	93.66	77.65
4	118.66	77.71
5	143.49	80.60
6	167.83	86.30
7	191.37	94.72
8	213.81	105.75
9	234.84	119.26
10	254.21	135.07
11	271.66	152.97
12	275.82	158.34

Circle Center At X = 105.6 ; Y = 297.3 and Radius, 220.0

*** 1.061 ***

Failure Surface Specified By 11 Coordinate Points

Point No.	X-Surf (ft)	Y-Surf (ft)
1	57.78	86.00
2	82.00	79.80
3	106.80	76.68
4	131.80	76.72
5	156.60	79.89
6	180.80	86.16
7	204.02	95.42
8	225.89	107.53
9	246.07	122.30
10	264.23	139.48
11	279.95	158.64

Circle Center At X = 119.0 ; Y = 274.7 and Radius, 198.4

*** 1.061 ***

Failure Surface Specified By 12 Coordinate Points

Point No.	X-Surf (ft)	Y-Surf (ft)
1	53.33	86.00
2	77.55	79.77
3	102.34	76.59
4	127.34	76.49
5	152.16	79.50
6	176.42	85.54
7	199.74	94.55
8	221.77	106.37
9	242.17	120.82
10	260.62	137.69
11	276.84	156.71
12	278.03	158.50

Circle Center At X = 115.6 ; Y = 277.8 and Radius, 201.7

*** 1.064 ***

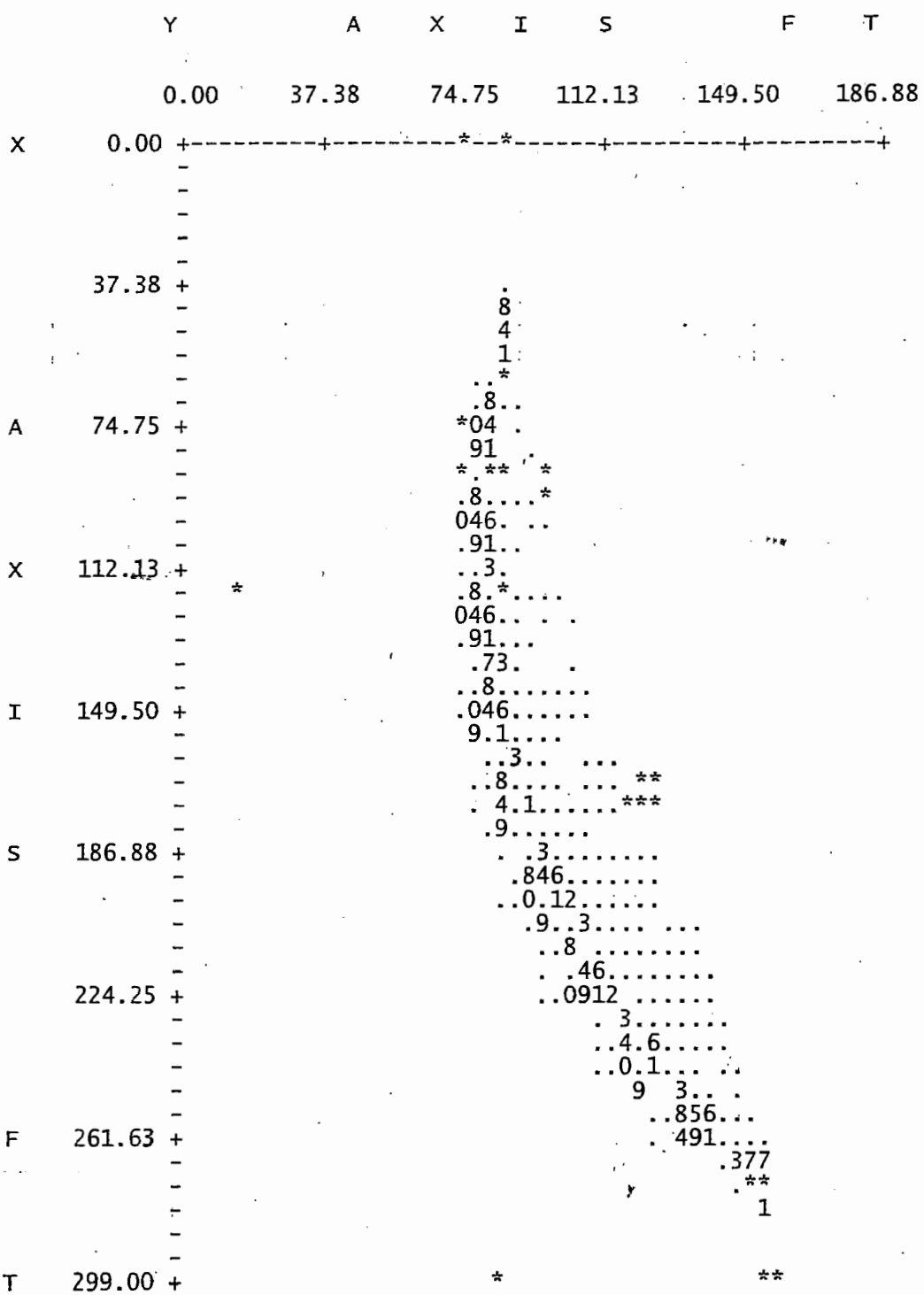

ENCLOSURE C

TO

ATTACHMENT 1

WASTE CONTAINMENT SYSTEMS, WASTE STABILIZATION, AND LANDFILLS: DESIGN AND EVALUATION

HARI D. SHARMA, PH.D., P.E.
Chief Engineer and Director
EMCON Associates
San Jose, California

SANGEETA P. LEWIS, P.E.
Project Manager
CH_2M Hill
Oakland, California

A Wiley-Interscience Publication
JOHN WILEY & SONS, INC.
New York / Chichester / Toronto / Brisbane / Singapore

TABLE 2.24 Strength Variation of Fly Ash and Mixtures of Fly Ash with Time

Material	q_u (kPa) 7 days	28 days
Michigan	0.170×10^3	0.210×10^3
New Jersey	0.310×10^3	0.425×10^3
UK	0.550×10^3	0.660×10^3
West Virginia		
Ash A with 3% lime	19.6×10^3	31.6×10^3
Ash A with 3% cement	7.4×10^3	12.8×10^3
Ash B with 3% lime	2.8×10^3	4.0×10^3
Ash B with 3% cement	3.2×10^3	8.0×10^3
Lignite fly ash (fly ash 10%, sand 90%)	2.6×10^3	4.6×10^3
Lime:fly ash:FDG sludge		
6.3:43.7:50.0	3.3×10^3	5.5×10^3
2.5:55.8:41.7	3.0×10^3	4.0×10^3
0:41.2:58.8	0.3×10^3	0.4×10^3
Fly ash:lime:cement:dredge waste		
4:0:0:96		8
0:4:0:96		10.5
0:0:4:96		38 = 5.5 psi = 794 psf
10:0:0:90		10
0:10:0:90		19
0:0:10:90		78 = 11.3 psi = 1630 psf

Source: Weis and Khera (1990). Reproduced by permission of Butterworth-Heinemann.

Oweis and Khera (1990) reviewed the results of strength tests performed by various investigators on mineral wastes. Evaluations indicated that addition of a small amount of lime or cement to fly ash may result in a strength increase. Table 2.23 summarizes strength properties of mineral wastes, and Table 2.24 presents strength variations of fly ash and mixtures of fly ash over time.

2.4.8 Compressibility

Compressibility of a municipal landfill is related to the settlement behavior of the landfill. However, unlike soils, the settlement behavior of a landfill is complex and can be influenced by various factors, such as movement of smaller particles into larger voids, chemical reactions, biodegradation of organics within the landfill, dissolving of soluble substances by percolating groundwater, creep, and changes in deformation properties with time (U.S. Dept. of the Navy, 1983; Sowers, 1968; Huitric 1981 and Fassett et al. 1994). Generally, it has been observed that a new landfill may settle up to 50 percent of its thickness or depth, while a closed landfill will settle between 15 and 20 percent of its total thickness after 10 to 15 years. Since landfill settlements vary significantly depending on specific waste types and